Development of a New Family of Conformationally Restricted Peptides as Potent Nucleators of β-Turns. Design, Synthesis, Structure, and Biological Evaluation of a β-Lactam Peptide Analogue of Melanostatin

Claudio Palomo,*,[†] Jesus M. Aizpurua,*,[†] Ana Benito,[†] José Ignacio Miranda,[†] Raluca M. Fratila,[†] Carlos Matute,[‡] Maria Domercq,[‡] Federico Gago,[§] Sonsoles Martin-Santamaria,[§] and Anthony Linden[‖]

Contribution from the Departamento de Química Orgánica I. Facultad de Química. Universidad del País Vasco. Apdo. 1072, 20080 San Sebastián, Spain

Received August 28, 2003; E-mail: qoppanic@sc.ehu.es

Abstract: Novel enantiopure (*i*)-(β-lactam)-(Gly)-(*i*+3) peptide models, defined by the presence of a central α-alkyl-α-amino-β-lactam ring placed as the (*i*+1) residue, have been synthesized in a totally stereocontrolled way by α-alkylation of suitable *N*-[bis(trimethylsilyl)methyl]-β-lactams. The structural properties of these β-lactam pseudopeptides have been studied by X-ray crystallography, Molecular Dynamics simulation, and NOESY-restrained NMR simulated annealing techniques, showing a strong tendency to form stable type II or type II′ β-turns either in the solid state or in highly coordinating DMSO solutions. Tetrapeptide models containing *syn*- or *anti*-α,β-dialkyl-α-amino-β-lactam rings have also been synthesized and their conformations analyzed, revealing that α-alkyl substitution is essential for β-turn stabilization. A β-lactam analogue of melanostatin (PLG amide) has also been prepared, characterized as a type-II β-turn in DMSO-d_6 solution, and tested by competitive binding assay as a dopaminergic D_2 modulator in rat neuron cultured cells, displaying moderate agonist activity in the micromolar concentration range. On the basis of these results, a novel peptidomimetic design concept, based on the separation of constraint and recognition elements, is proposed.

Introduction and Objectives

Turns, defined as sites where a peptide chain reverses its overall direction, are common motifs in protein structures.[1] When direction reversal occurs over four residues in such a way that the carbonyl oxygen atom of the first residue (*i*) and the amide NH proton of the fourth residue (*i*+3) come close to each other in space, a β-turn is formed.[2] Furthermore, in the case of β-turns of types I, II and III, this conformation involves formation of an intramolecular hydrogen bond between residues (*i*) and (*i*+3) to give a pseudo-10-membered ring.[3] From a structural chemistry viewpoint, β-turns are critical to protein conformational stability[4] and many protein−protein interactions.[5] In addition, turns are often a preferred site for degradation by proteolytic enzymes.[6] Hence, it is not surprising that β-turn-

based pharmacophore design has become a central topic in medicinal chemistry.[7]

Synthesis of molecular templates for β-turns with precisely oriented predetermined groups is a complex task, and a great deal of effort has been dedicated to the development of such peptidomimetics.[6,8] Basically, a rational design of an efficient mimetic requires the formal modification of the native bioactive peptide to include two elements. First, a specific β-turn

---

[†] Universidad del País Vasco.

[‡] Biological assays: Departamento de Neurociencias, Facultad de Medicina, Universidad del País Vasco, 48940 Leioa, Spain.

[§] MD calculations: Departamento de Farmacología. Facultad de Medicina. Universidad de Alcalá de Henares. 28871 Madrid, Spain.

[‖] X-ray crystallography: Organisches-chemisches Institut der Universität Zürich. Winterthurerstrasse 190, CH-8057, Zürich, Switzerland.

(1) For a classification of turns, see: Wilmot, C. M.; Thornton, J. M. *Protein Eng.* **1990**, *3*, 479−493.

(2) Reviews: (a) Rizo, J.; Gierasch, L. M. *Annu. Rev. Biochem.* **1992**, *61*, 387. (b) Rose, G. D.; Gierasch, L. M.; Smith, J. A. *Adv. Protein Chem.* **1985**, *37*, 1−109. (c) Schneider, J. P.; Kelly, J. W. *Chem. Rev.* **1995**, *95*, 2169−2187. (d) Serrano, L. *Adv. Protein Chem.* **2000**, *53*, 48−85.

(3) Four essential structural parameters define canonical β-turns: (a) donor/acceptor distance $_{(i+3)}$NH⋯O=C$_{(i)}$ of the turn-stabilizing hydrogen bond (typically, 1.8−2.5 Å for H⋯O distance and 2.6−3.2 Å for N⋯O distance); (b) the Cα$_{(i)}$−Cα$_{(i+3)}$ distance (<7 Å); (c) pseudodihedral angle δ encompassing four consecutive Cα atoms of the turn-forming amino acids (ideal value: 50° > δ > −50°); (d) φ and ψ dihedral angle sets at the −(*i*+1)−(*i*+2)− positions. See: (a) Robinson J. A. *Synlett* **2000**, *4*, 429−441. (b) Müller, G.; Hessler, G.; Decornez, H. Y. *Angew. Chem., Int. Ed.* **2000**, *39*, 894−896.

(4) (a) Northup, S. H.; Pear, M. R.; Morgan, J. D.; McCammon, J. A.; Karplus, M. *J. Mol. Biol.* **1981**, *153*, 1087−1109. (b) Jaskólski, M.; Tomasselli, A. G.; Sawyer, T. K.; Staples, D. G.; Heinrikson, R. L.; Schneider, J.; Kent, S. B. H.; Wlodawer, A. *Biochemistry* **1991**, *30*, 1600−1609.

(5) For a review, see: Burgess, K. *Acc. Chem. Res.* **2001**, *32*, 826−835.

(6) For detailed information on this subject: Arnold, U.; Hinderaker, M. P.; Nilsson, B. L.; Huck, B. R.; Gellman, S. H.; Raines, R. T. *J. Am. Chem. Soc.* **2002**, *124*, 8522−8523.

(7) For a review, see: Souers, A. J.; Ellman, J. A. *Tetrahedron* **2001**, *57*, 7431−7448.

(8) General reviews on peptidomimetic synthesis: (a) Synthesis of Peptides and Peptidomimetics. In *Houben-Weyl, Methods of Organic Chemistry*; Felix, A., Moroder, L., Toniolo, C., Eds.; Thieme: Stuttgart, New York, 2003; Vol. E22c. (b) Hanessian, S.; McNaughton-Smith, G.; Lombart, H.-G.; Lubell, W. D. *Tetrahedron* **1997**, *53*, 12789−12854. (c) Gante, J. *Angew. Chem., Int. Ed. Engl.* **1994**, *33*, 1699−1720. (d) Giannis, A.; Kolter, T. *Angew. Chem., Int. Ed. Engl.* **1993**, *32*, 1244−1267.
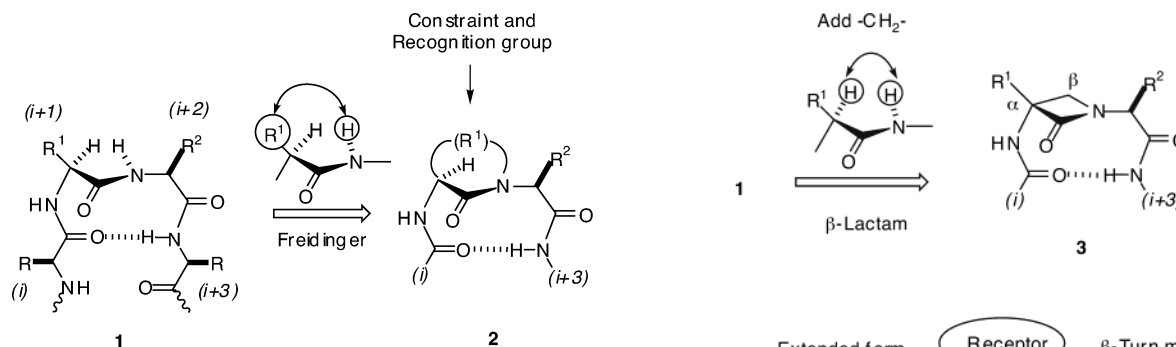
Figure 1. Freidinger's basic principle for β-turn peptidomimetic design.

constraining element (e.g., an intra- or interresidual bridge) is needed to force the peptide backbone to overlay the desired conformation as exactly as possible. Second, at least one recognition group must be placed in a stereocontrolled and synthetically easy way at the desired position for interaction with the receptor or enzyme active site. Though formally simple at a design level, practical access to peptidomimetic libraries bearing a broad range of recognition groups, while retaining the β-turn framework, often conflicts with the synthetic reliabilities arising from the structure of the scaffolds chosen. Indeed, it is difficult or impossible to elucidate structural elements exerting specific constraints or recognition functions for most known β-turn surrogate molecules. As a consequence, chemical alteration of such peptidomimetics, when synthetically feasible, leads to unpredictable results in terms of β-turn motif stability and/or proper spatial orientation of the recognition groups. An important example of this phenomenon (Figure 1) is the original approach of Freidinger[9] to β-turn mimetics, involving the bridging of the betagenic $-(i+1)-(i+2)-$ central residues through the formation of five-, six-, seven-, and eight-membered ring lactams **2**. Accordingly, any structural modification of the R^1 bridge in pseudopeptide **2**,[10] should force a global change of conformation and recognition properties that, in practice, involves a re-design of each derivative prepared, instead of a single structural parameter variation.

The objective of this work is to propose a novel design approach to β-turn peptidomimetics based on the principle of the incorporation of groups, as small as possible, in the original peptide to generate well-defined turns without affecting receptor recognition. Herein we report in detail our investigation of the design, synthesis, conformational characterization and biological evaluation of a novel β-lactam peptide analogue of melanostatin (PLG) that illustrates this concept. In addition, the identification of the structural parameters involved in the stabilization of β-lactam-based peptidomimetics as a novel family of β-turn motif nucleators is also reported.

Results and Discussion

β-Lactam Peptide Design Plan. Our idea is based upon consideration (Figure 2) that a methylene bridge between the $C\alpha_{(i+1)}$ and the $N_{(i+2)}$ atoms in peptide **1** should mimic
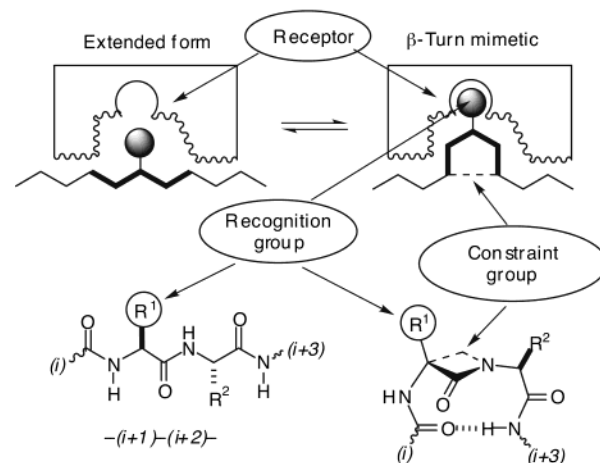
(9) (a) Freidinger, R. M.; Veber, D. F.; Perlow, D. S.; Brooks, J. R.; Saperstein, R. *Science* **1980**, *210*, 656−658. (b) Freidinger, R. M.; Schwenk, D.; Veber, D. F. *J. Org. Chem.* **1982**, *47*, 104−109. (c) Freidinger, R. M. *J. Org. Chem.* **1985**, *50*, 3631−3633.
(10) For reviews on conformationally restricted peptides through short-range cyclizations, see: (a) Toniolo, C. *Int. J. Peptide Protein Res.* **1990**, *35*, 287−300. (b) Liskamp, R. M. J. *Recl. Trav. Chim. Pays-Bas* **1994**, *113*, 1−19.

Figure 2. Principles for the design of a novel class of peptidomimetics as nucleators of β-turn motifs: when the β-lactam methylene group mimics simultaneously the $C\alpha H_{(i+1)}$ and $HN_{(i+2)}$ protons of the native peptide, R^1 and R^2 groups can be designed specifically for recognition with the receptor.

simultaneously the $C\alpha H_{(i+1)}$ and $HN_{(i+2)}$ protons of the native peptide with a minimal structural divergence,[11] thus retaining the R^1 α substituent of the original residue and facilitating a closer recognition by receptors or enzymes. From this design, a four membered ring with a quaternary stereogenic center at the $C\alpha$ position results as a key element. In this approach, it was also assumed that the presence of the α,α-disubstitution pattern would enhance resistance to chemical and enzymatic hydrolysis by proteases[12] and that the resulting β-lactam-peptides **3** would be attractive targets for pharmaceutical drug discovery.

The major difficulty in the development of β-lactam peptides stems from the lack of methodology to create the α-quaternary stereogenic center in β-unsubstituted azetidin-2-one rings.[13] We recently addressed this issue[14] (Scheme 1) and found that the asymmetric alkylation of the β-lactam **4** proceeds with control of the configuration at the C_3 position being dictated by the stereogenic center of the oxazolidinone moiety to give the α-amino-α-substituted products with high yields and excellent

(11) It has been reported that the $C\alpha H_{(i+1)}$ to $HN_{(i+2)}$ interproton distance is an essential parameter to differentiate type-I and type-II β-turns. For instance, in Ac-Pro-Gly-Me model peptide the $_{(Pro)}C\alpha H\cdots HN_{(Gly)}$ distance is 3.5 Å for a type-I β-turn, but only 2.1 Å for type-II conformation; see: Narasinga Rao, B. N.; Kumar, A.; Balaram, H.; Ravi, A.; Balaram, P. *J. Am. Chem. Soc.* **1983**, *105*, 7423−7428.
(12) Detailed information on this subject: (a) *The Chemistry of β-Lactams*; Page, M. I., Ed.; Blackie Academic & Professional: New York, 1992. (b) *Chemistry and Biology of β-Lactam Antibiotics*; Morin, R. B., Gorman, M., Eds.; Academic: New York, 1982; Vols. 1−3. (c) *The Organic Chemistry of β-Lactams*; Georg, G. I., Ed.; VCH: New York, 1993.
(13) For a general review on β-lactam synthesis, see: Backes, J. In *Houben-Weyl, Methoden der Organischen Chemie*; Muller, E., Bayer, O., Eds.; Thieme: Stuttgart, 1991; Band E16 B, p 31.
(14) (a) Palomo, C.; Aizpurua, J. M.; Galarza, R.; Benito, A.; Khamrai, U.K.; Eikeseth, U.; Linden, A. *Tetrahedron* **2000**, *56*, 5563−5570. (b) Palomo, C.; Aizpurua, J. M.; Benito, A.; Galarza, R.; Khamrai, U.K.; Vazquez, J.; DePascual-Teresa, B.; Nieto, P. M.; Linden, A. *Angew. Chem., Int. Ed.* **1999**, *38*, 3056−3058.

Scheme 1. (Top) Synthesis of β-Lactam Peptidomimetic **6**. (Bottom) Main Structural Parameters of β-Lactam Peptidomimetic **6** in the Solid State (X-ray Crystal Structure)[a]

(ref. 14)
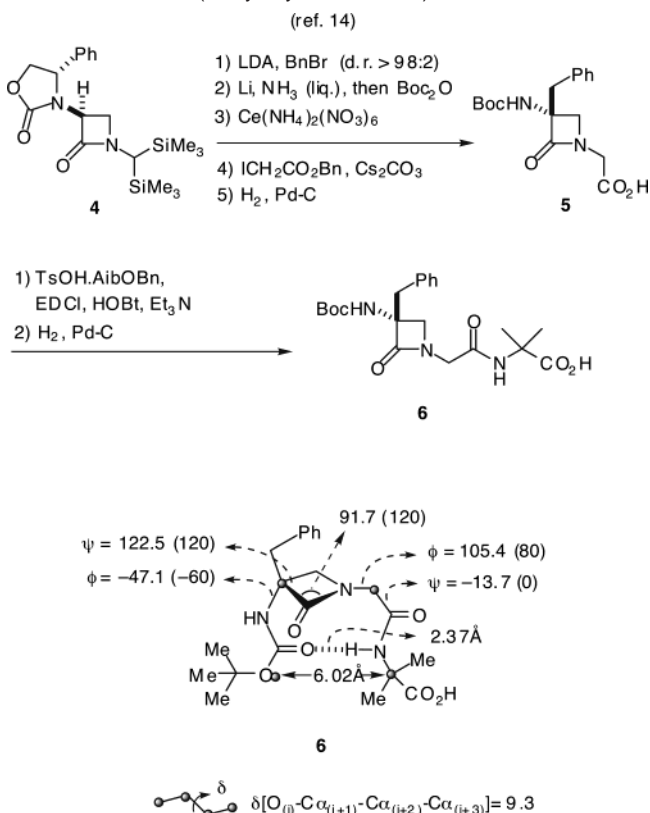
[a] Key: EDCl = 1-(3-dimethylaminopropyl)-3-ethylcarbodiimide hydrochloride; HOBt = 1-hydroxybenzotriazole; TsOH = *p*-toluenesulfonic acid. Ideal values indicated in parentheses.

diastereoselectivities. This approach, after deprotection of the bis(trimethylsilyl)methyl moiety with cerium(IV) ammonium nitrate in the resulting alkylated products and incorporation of the carboxymethyl group at the nitrogen atom, allows access to the required β-lactam scaffolds (e.g., **5**), which can be coupled at the N- and C-termini through conventional peptide synthesis.

At the outset of our investigation, however, it was not evident which sort of conformation would adopt such β-lactam peptides. Actually, the incorporation of β-lactam scaffolds into peptide backbones has virtually been ignored[15] and structural information regarding the conformation of the resulting peptide isosters is very limited.[16] We were pleased to find that the first β-lactam peptide (**6**) prepared using this approach presented some remarkable structural features. For example, as deduced from the X-ray crystal structure,[14b] the lactam carbonyl C−CO−N angle was 91.7(2)°, considerably smaller than in parent peptides (∼120°). The distance between the C_3 and N_1 atoms in the β-lactam ring (2.085(5) Å) was also about 0.4 Å shorter than in the ideal type II β-turn segment ($C\alpha_{(i+1)}\cdots N_{(i+2)} \approx 2.48$ Å).

Moreover, the pseudodihedral angle[17] spanned by the four Cα atoms in the ideal type II β-turn (∼0°) was correctly mimicked (9.3(2)°) by the sequence formed by the ${}^tBuO$ oxygen atom, the Cα of the β-lactam ring, and the two Cα atoms of the glycine and Aib residues, respectively. Furthermore, the C=O⋯H−N hydrogen bond distance (2.37(3) Å) and the O⋯H−N angle (167(3)°) indicated the presence of an intramolecular interaction which, on the basis of the φ and ψ dihedral angle sets at the −(*i*+1)-(*i*+2)− positions, defined a type-II β-turn distorted by ∼15−25° at $\phi_{(i+1)}$, $\phi_{(i+2)}$, and $\psi_{(i+2)}$. Solution conformational analysis (NMR) of **6** in noncoordinating solvents (CDCl₃) assessed the presence of a single type-II β-turn conformer at room temperature, essentially similar to that observed in the solid state.

In general, it is assumed that the betagenic bias of tetrapeptide segments constrained by inter-residual lactams is primarily determined by the central −(*i*+1)-(*i*+2)− pair and only partially stabilized by N- and C-terminal residues. Consequently, with the aim of establishing whether our β-turn design would be general in scope, different enantiopure tetrapeptide models **7** (Figure 3) incorporating a central −(β-lactam)-(Gly)− pair and achiral (*i*) and (*i*+3) termini were selected for development. The insertion of glycine, the most flexible α-amino acid, in the central (*i*+2) position was intentionally devised to prevent any masking influence of the chiral residue on the constraining effect of the azetidin-2-one ring. The first obvious question we addressed was to determine whether the quaternary center at the C_3 position of the azetidin-2-one ring would be essential for conformational restriction or not. To this end, the β-lactam-based peptide **8** was envisaged for comparison with the above C_3 benzyl-substituted peptide **6**. To simplify the solution NMR analysis, Boc[18] and Aib groups were chosen, respectively, as the (*i*) and (*i*+3) residues to provide singlet methyl signals in the high field region, which would not interfere with the amide NH region. Then, to rule out any possible specific influence of the terminal Boc and Aib residues on the betagenicity of −(β-lactam)-Gly− fragments, a β-lactam peptide **9** flanked by fully flexible (*i*), (*i*+2), and (*i*+3) glycine residues was also devised.

In addition to the above issues, the substitution pattern at the C_4 position of the β-lactam ring is another concern relevant to our design. In this instance, four diastereomeric β-lactams may be formed and their relative configuration at the C_3 and C_4 positions might influence the configurational behavior of the corresponding tetrapeptide. To evaluate this question, β-lactam peptides **10** and **11** with the 3,4-dialkyl substituents in a *syn*- and *anti*-relationship, respectively, were selected as models for the study.

On the other hand, melanostatin or L-prolyl-L-leucylglycinamide (PLG) **12**, an endogenous brain peptide of hypothalamic origin possessing a type-II β-turn bioactive conformation, was selected as a parent peptide to illustrate the "proof-of-principle" of the proton mimic design strategy. This molecule is associated with the modulation of dopaminergic D₂ membrane receptors in the central nervous system,[19] and owing to its neuroprotecting properties, many conventional lactamic, spirolactamic, and

(15) β-Amino-desacetoxycephalosporanic acid oligopeptides have been show to present weak in vitro inhibitory activity against porcine pancreatic elastase, α-chymotrypsin and human immunodeficiency virus type 1 proteinase (HIV-1 PR): (a) Pitlik, J.; Bassogi, P.; Jeko, J.; Tozser, J. *Pharmazie* **1996**, *51*, 700−704.

(16) Concurrent with our investigation, Alonso and Gonzalez have shown by NMR studies that racemic spiro β-lactams derived from Boc-prolyl chloride and benzaldehyde imines are able to adopt regular type II β-turn mimetics which are stable in CDCl₃ solution but collapse in DMSO-*d₆*. (a) Alonso, E.; López-Ortiz, F.; Del Pozo, C.; Peralta, E.; Macías, A.; González, J. *J. Org. Chem.* **2001**, *66*, 6333−6338. See also: (b) Linder, M. R.; Podlech, J. *Org. Lett.* **1999**, *1*, 869−871.

(17) Such a pseudodihedral angle has been proposed to be relevant to distinguish type-II′ and type-I β-turns, see: Müller, G. *Angew. Chem., Int. Ed. Engl.* **1996**, *35*, 2767−2769.

(18) The Boc group has been proposed as a N-terminal residue mimic that does not affect the conformational behavior of short peptides, see: Shaw, R. A.; Perczel, A.; Fasman, G. D.; Mantsch, H. H. *Int. J. Peptide. Res.* **1996**, *48*, 71−78.
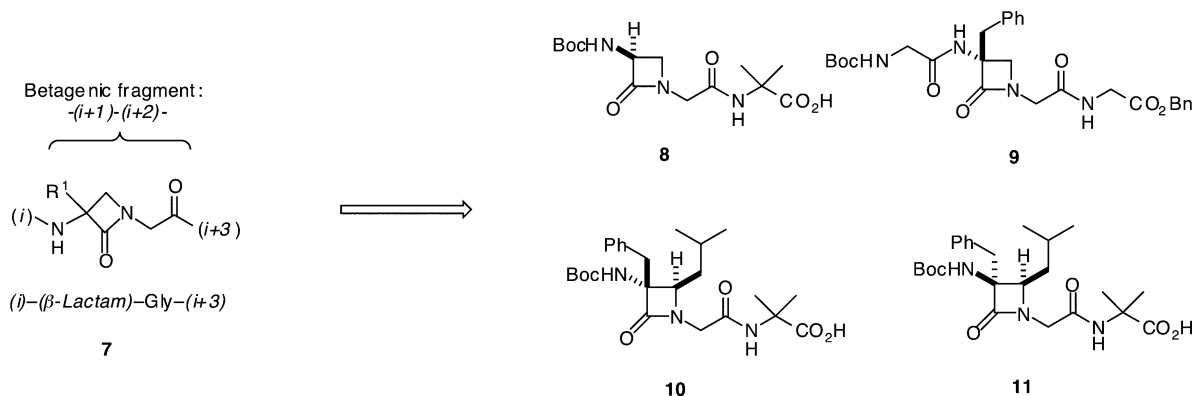
Figure 3. Representative tetrapeptide models **8**−**11** as a function of the structural and stereochemical elements of the β-lactam core for β-turn induction.
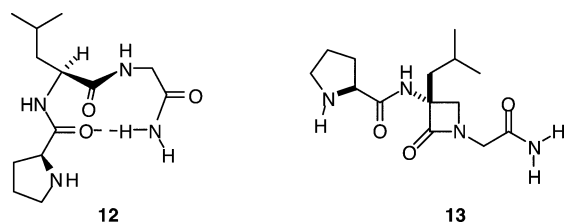

Figure 4. Melanostatin **12** and peptidomimetic analogue **13** derived from our proton mimic design strategy.

policyclic peptidomimetics[20] of PLG have been developed during the past decades as potential new drugs against Parkinson's disease or tardive diskynesia. Application of the β-lactam peptidomimetic approach[21] naturally leads to the mimetic **13**. An assessment of the type-II β-turn conformation for this peptide model in water or highly coordinating solvents, together with its biological activity retention with respect to PLG, would provide evidence that the β-lactam methylene group can, indeed, mimic $C\alpha H_{(i+1)}$ and $HN_{(i+2)}$ protons.

β-Lactam Peptide Synthesis. Oligopeptides **8** and **9**, containing β-lactams unsubstituted at the C_4 position of the ring, were prepared uneventfully from a single *N*-[bis(trimethylsilyl)-methyl]-β-lactam precursor **4** (Scheme 2). Accordingly, sequential deprotection of the 4-phenyloxazolidinone and bis-(trimethylsilyl)methyl moieties under the same conditions used for the preparation of **6** (Scheme 1) furnished the enantiomerically pure NH-β-lactam **14**[22] in 76% overall yield, which was directly subjected to chemoselective carboxymethylation at the β-lactam nitrogen atom in the presence of cesium carbonate, using the Miller's method,[23] followed by hydrogenolysis to the free acid **15**. Coupling of fragment **15** with α-aminoisobutiric acid benzyl ester, carried out under homogeneous conditions using the water-soluble carbodiimide method,[24] (EDCl)/1-

Scheme 2. Synthesis of Model Peptides **8** and **9**
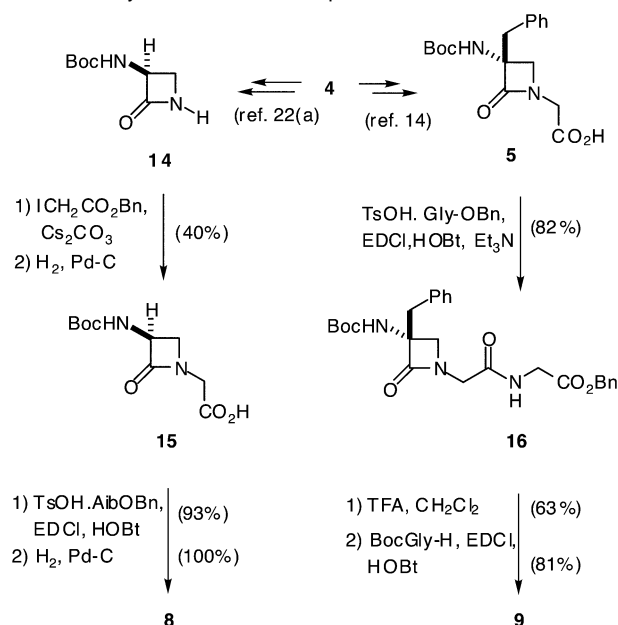
hydroxybenzotriazole (HOBt), afforded peptidomimetic **8** as a microcrystalline solid. Similarly, the 3-benzyl-*N*-carboxymethyl substituted analogue **5**, upon sequential double-glycine coupling in the C- and N-terminal positions, provided **9** in 42% overall yield.

Tetrapeptides **10** and **11** were also prepared in a similar way as shown in Scheme 3. At the outset, however, it was not clear which synthetic route would be best suited for the preparation of the α-amino-α,β-dialkyl β-lactam core of each peptide product. Apparently, the most direct access to these compounds would also be the asymmetric alkylation of α-amino β-lactams, a technology established by Ojima almost 20 years ago.[25] However, from this strategy, only one isomer β-lactam product with the C_3 and C_4 groups in an *anti*-relationship is accessible. We adopted this approach starting from β-lactam **17** (Scheme 3), easily prepared in 70% yield via the cycloaddition reaction of Evans' ketene, with the imine derived from isobutiraldehyde and C,C-bis(trimethylsilyl)methylamine[26] and have found that, contrary to all expectations, the alkylation of the lithium enolate of **17** with benzyl bromide provided the *syn*-3,4-dialkyl β-lactam

(19) For a review of the biological activities of PLG: Mishra, R. K.; Chiu, S.; Mishra, C. P. *Methods Find. Exptl. Clin. Pharmacol.* **1983**, *5*, 203−233.

(20) (a) Evans, M. C.; Johnson, R. L. *Tetrahedron* **2000**, *56*, 9801−9808. (b) Webber, K.; Ohnmacht, U.; Gmeiner, P. *J. Org. Chem.* **2000**, *65*, 7406−7416. (c) Baures, P. W.; Pradhan, A.; Ojala, W. H.; Gleason, W. B.; Mishra, R. K.; Jonson, R. L. *Bioorg. Med. Chem. Lett.* **1999**, *9*, 2349−2352. (d) Baures, P. W.; Ojala, W. J.; Costain, W. J.; Ott, M. C.; Gleason, W. B.; Mishra, R. K.; Johnson, R. L. *J. Med. Chem.* **1997**, *40*, 3594−3600.

(21) The β-turn empirical assignment for a β-lactam analogue of Pro-Leu-Gly-NH₂ has been reported on the basis of competitive binding enhancement on D₂ dopaminergic receptors in the presence of agonist [³H]ADTN: Sreenivasan, U.; K.Mishra, R.; Johnson, R. L. *J. Med. Chem.* **1993**, *36*, 256−263.

(22) (a) Palomo, C.; Aizpurua, J. M.; Legido, M.; Galarza, R. *Chem. Commun.* **1997**, 233−234. Alternatively, this compound could also be prepared from *N*-Boc-L-serine using Millers' hydroxamate method in 67% yield; see: (b) Mattingly, P. G.; Miller, M. J. *J. Org. Chem.* **1980**, *45*, 410−415.

(23) Guzzo, P. R.; Miller, M. J. *J. Org. Chem.* **1994**, *59*, 4862−4867.

(24) Carpino, L. A.; El-Faham, A. *Tetrahedron* **1999**, *55*, 6813−6830.

(25) (a) Ojima, I. *Acc. Chem. Res.* **1995**, *28*, 383−389. (b) Ojima, I. In *The Organic Chemistry of β-Lactams*; Georg, G. I., Ed.; VCH: New York, 1992; p 197.

Scheme 3. Synthesis of Peptidomimetic Models **10** and **11**
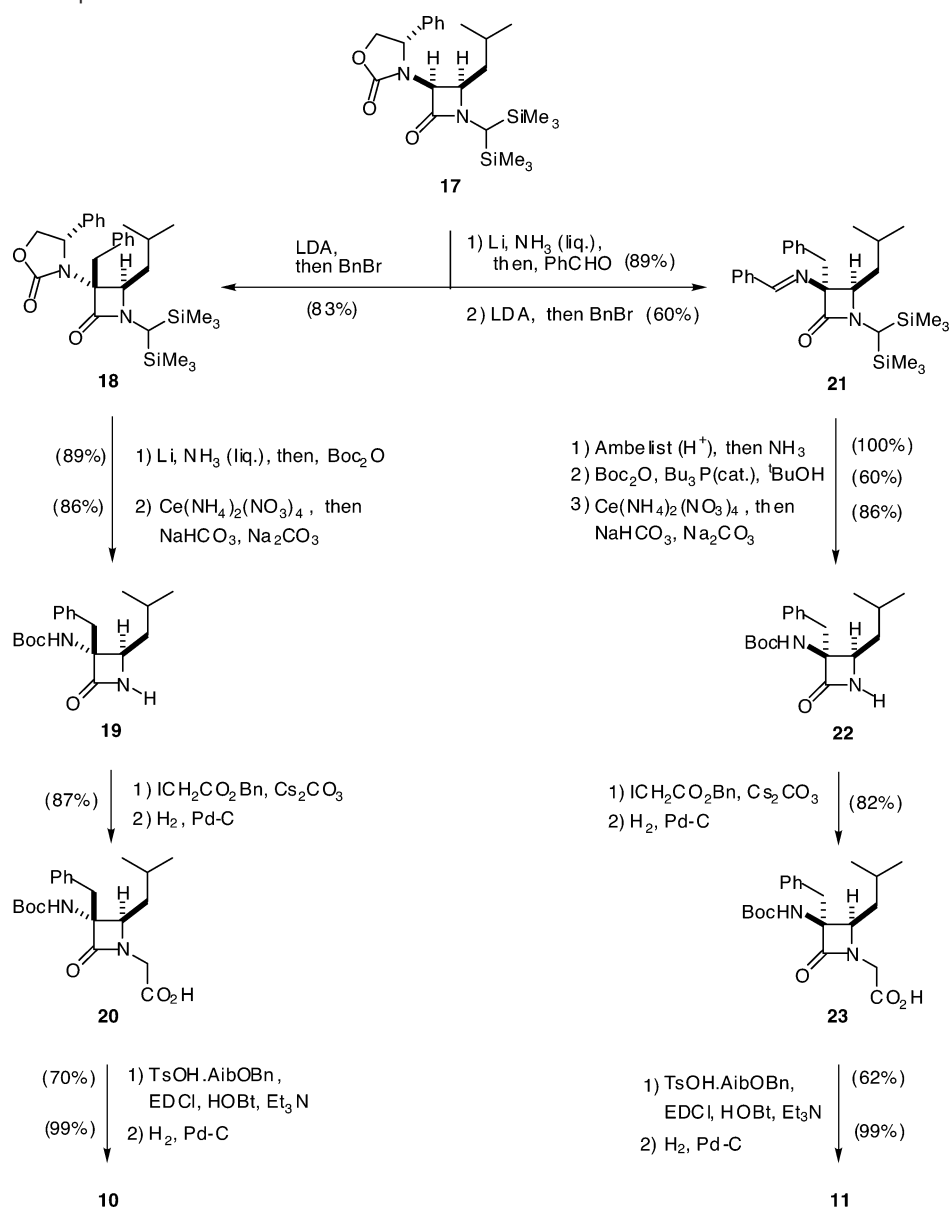
18[27] essentially as single diastereomer. Compound **18** was freed of the oxazolidinone group by metal-reduction with lithium in liquid ammonia and of the bis(trimethylsilyl)methyl group by a Ce(IV) oxidation reaction, giving rise to the NH-β-lactam **19** which was submitted to an identical N-carboxymethylation reaction and peptide coupling as compound **14** (Scheme 2), thereby affording *syn*-α,β-dialkyl substituted β-lactam peptidomimetic **10** in 60% overall yield. Concurrently, it was found that the preparation of the β-lactam **22** with the C_3 and C_4 substituents in an *anti*-relationship, needed for peptidomimetic **11**, could be realized upon exchange of the oxazolidinone ring in **17** by a benzaldehyde-imine group. In this instance, the

alkylation of the intermediate enolate proceeded under stereo-control dictated by the substituent at the C_4-position[28] to give **21** in 60% yield and essentially as the sole diastereomeric product. Hydrolysis of imine **21** was unusually difficult, but upon exposure to strongly acidic Amberlyst resin in moist diethyl ether solution, followed by basic treatment with ammonia provided the desired α-amino-β-lactam quantitatively. Protection of the latter as a *tert*-butyl carbamate also proved difficult under ordinary conditions (ditertbutyl dicarbonate in acetonitrile), but could finally be achieved by means of a variation of the method of Knölker using tributylphosphine as promoter.[29] Further elaboration to the desired peptidomimetic model **11** was carried out similarly to its diastereomer **10**.
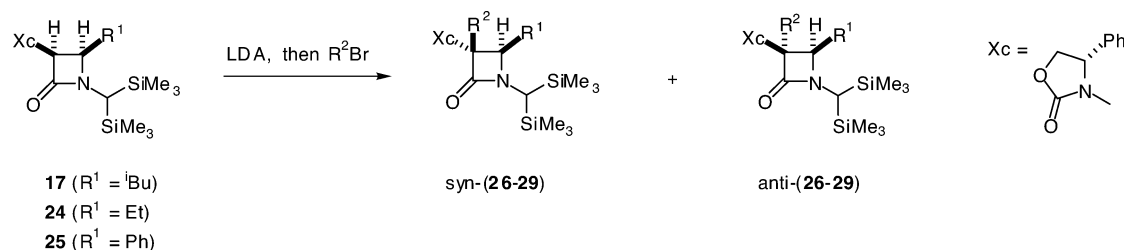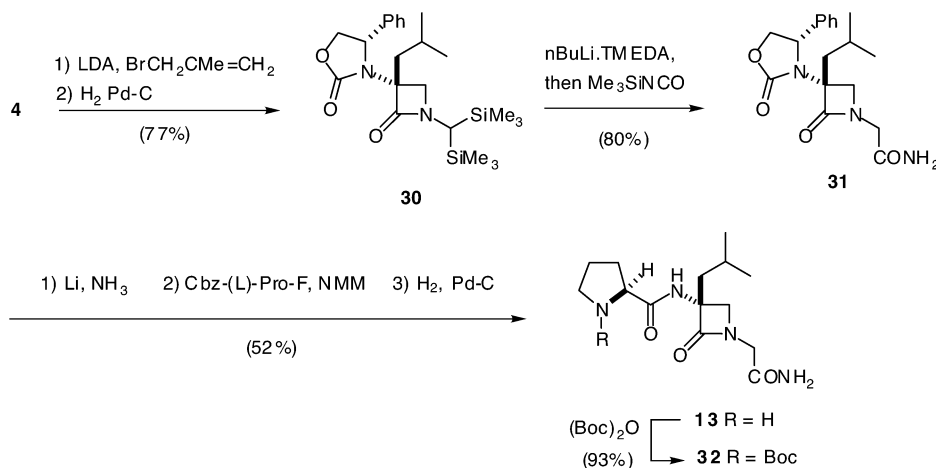
At this stage and, in view of the results noted above, it was judged instructive to get some further insight into the scope of

(26) Direct access to enantiomerically pure 3-amino-4-alkyl-substituted β-lactams from enolizable aldehyde-derived imines is not obvious. For a solution to this problem through the ketene—imine Staudinger cycloaddition reaction using *N*-bis(trimethylsilyl)methyl imines, see: (a) Palomo, C.; Aizpurua, J. M.; Legido, M.; Galarza, R.; Deya, P. M.; Dunogues, J.; Picard, J. P.; Ricci, A.; Seconi, G. *Angew. Chem., Int. Ed. Engl.* **1996**, *35*, 1239−1241. (b) Palomo, C.; Aizpurua, J. M.; Legido, M.; Mielgo, A.; Galarza, R. *Chem. Eur. J.* **1997**, *3*, 1432−1441 and references therein.

(27) The configuration of compound **18** was ascertained by X-ray crystallographic analysis; see the Supporting Information.

(28) Ojima, I.; Chen, H.-J. C.; Nakahashi, K. *J. Am. Chem. Soc.* **1988**, *110*, 278−281.

(29) (a) Knölker, H.-J.; Braxmeier, T.; Schlechtingen, G. *Angew. Chem., Int. Ed. Engl.* **1995**, *35*, 2497−2500. (b) Knölker, H.-J.; Braxmeier, T. *Tetrahedron Lett.* **1996**, *37*, 5861−5864.

Scheme 4. α-Alkylation of C₄-Substituted *N*-[Bis(trimethylsilyl)methyl]-β-lactam Peptidomimetic

17 (R¹ = ^iBu)
24 (R¹ = Et)
25 (R¹ = Ph)

syn-(**26-29**)   +   anti-(**26-29**)

Xc =

Scheme 5. Synthesis of PLG β-Lactam Peptidomimetic **13**[a]

4

1) LDA, BrCH₂CMe=CH₂
2) H₂ Pd-C
(77%)

30

nBuLi·TMEDA,
then Me₃SiNCO
(80%)

31

1) Li, NH₃   2) Cbz-(L)-Pro-F, NMM   3) H₂, Pd-C
(52%)

(Boc)₂O
(93%)

13 R = H
32 R = Boc

[a] TMEDA = *N,N,N′,N′*-tetramethylethylenediamine.

Table 1. *Syn*-Stereoselective Alkylation of C₄-Substituted *N*-[Bis(trimethylsilyl)methyl]-β-lactams **17**, **24**, and **25**

product	R¹	R²	yield[a] (%)	syn/anti[b]	$[\alpha]^{25}_D$ (c = 1.0, Cl₂CH₂)[c]
26	^iBu	CH₂=CHCH₂–	84	67:33	−4.6
27	Et	4-BrC₆H₄CH₂–	60	>98:2	−6.8
28	Ph	CH₂=C(Me)CH₂–	67	93:7	−54.5
29	Ph	4-MeC₆H₄CH₂–	90	92:8	−74.7

[a] Isolated yield of the mixture of *syn*- and *anti*-α,β-dialkyl-β-lactams. [b] Determined by ¹H NMR (500 MHz) analysis of the reaction crude. Stereochemical assignments confirmed by X-ray crystal structure analyses and/or NMR(NOE) spectroscopy. [c] Data corresponding to the pure *syn*-isomer.

the *syn*-selective alkylation of *N*-[bis(trimethylsilyl)methyl]-β-lactams (Scheme 4, Table 1). It was found that, indeed, the alkylation reaction of β-lactams **17**, **24**, and **25** with both allyl and benzyl halides proceeds under high levels of stereocontrol to give α-alkylated products in excellent syn/anti selectivity ratios. Most notably, although the precise control elements that govern these reactions are not clear at present, the results appear to be quite regular regardless of the substituent at the C₄ position of the β-lactam ring. Since the stereochemical outcome of these reactions may be reversed upon exchange of the oxazolidinone ring, vide supra, our approach enables access to both syn- and anti-α-amino-α,β-dialkyl-β-lactams starting from a single β-lactam product, a feature of the approach that may also be of general interest in the chemistry of β-lactams.

On the other hand, for the reasons that we have outlined earlier, vide supra, the β-lactam peptide analogue of melanostatin was prepared from the β-lactam **4** via alkylation with methallyl bromide, subsequent catalytic hydrogenation and finally installation of the proline and glycinamide residues as shown in Scheme 5. In this instance, it was found that introduction of

the glycinamide residue could be performed by treatment of **30** with 1.2 equiv of preformed *n*-BuLi/TMEDA complex at −100 °C in THF and subsequent trapping of the lithiated intermediate with trimethylsilyl isocyanate.[30] Conventional peptide coupling of the resulting **31** with Cbz-protected L-proline using the EDCl/HOBt method proved inefficient, and only 25−35% yields of the expected peptide were obtained after repeated runs. This poor conversion, which was attributed to the combined steric hindrance of the β-lactam amine and the activated Cbz-proline/HOBt intermediate, was finally improved using Carpino's amino acid fluoride method.[31] Thus, coupling of the α-amino-β-lactam derived from **31** with "in situ" formed Cbz-Pro-F in the presence of *N*-methylmorpholine (NMM) followed by hydrogenolytic debenzylation led to **13** in 52% overall yield. The PLG analogue **13** was a thick colorless oil, but proper single crystals for X-ray crystallographic analysis were grown from solutions of its *N*-Boc-protected form **32**.

Solid-State Structures. After intensive trials, only compounds **6**,[14b] **11**, and **32**, the *N*-Boc derivative of **13**, afforded suitable single crystals for crystallographic analysis (see the

(30) Only deprotonation at the C*H*(SiMe₃)₂ methine group was observed. Apparently, the known "α-silicon effect" in conjunction with a considerable "complex-induced proximity effect" (CIPE) between the sterically α-blocked β-lactam carbonyl oxygen lone pair and lithium cation are responsible for the deprotonation at this position and not at the methylene group. For reviews on the α-silicon effect, see: (a) Itami, K.; Kamei, T.; Mitsudo, K.; Nokami, T.; Yoshida, J.-I. *J. Org. Chem.* **2001**, *66*, 3970−3976. (b) Panek, J. S. Silicon Stabilization. In *Comprehensive Organic Synthesis*; Trost, B. M., Fleming, I., Eds.; Pergamon: New York, 1991; Vol. 1, p 579. For surveys on CIPE, see: (c) Beak, P.; Meyers, A. I. *Acc. Chem. Res.* **1986**, *19*, 356−363. (d) Snieckus, V. *Chem. Rev.* **1990**, *90*, 879−933. (e) Beak, P.; Basu, A.; Gallagher, D. J.; Park, Y. S.; Thayumanyan, S. *Acc. Chem. Res.* **1996**, *24*, 552−560. (f) Hoveyda, A. H.; Evans, D. A.; Fu, G. C. *Chem. Rev.* **1993**, *93*, 1307−1370. An extention of the scope of this reaction to other *N*-[bis(trimethylsilyl)methyl]-β-lactams is currently underway in our laboratory.
(31) Carpino, L. A.; Mansour, E.-S. M. E.; Sadat-Aalaee, D. *J. Org. Chem.* **1991**, *56*, 2611−2614.

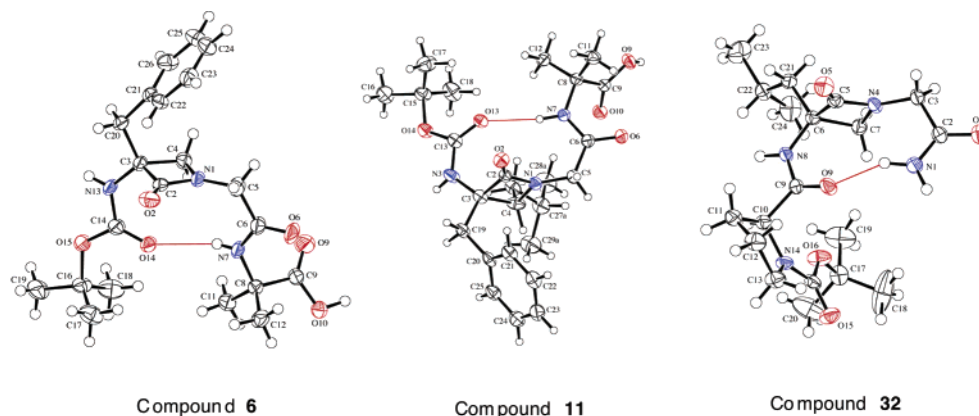Compound **6**   Compound **11**   Compound **32**

Figure 5. ORTEP plots of the molecular structures of compounds **6**, **11**, and **32**, showing β-turned conformations (only one of the two symmetry-independent molecules in the asymmetric unit of **6** is shown).

Table 2. Selected Geometric Parameters for β-Lactam Peptidomimetics in the Solid State

compd	$_{(i)}C{=}O{\cdots}HN_{(i+3)}$ (Å)	$\phi_{(i+1)}$; $\psi_{(i+1)}$ (deg)	$\phi_{(i+2)}$; $\psi_{(i+2)}$ (deg)	$C\alpha_{(i)}{\cdots}C\alpha_{(i+3)}$ (Å)	δ (deg)^b	$_{(i)}O{\cdots}H{-}N_{(i+3)}$ (deg)
6 (A)^a	2.32(3)	−40.9(5); 122.5(3)	100.5(4); −2.1(5)	5.957(5)	17.5(2)	164(3)
6 (B)^a	2.37(3)	−47.1(4); 122.5(3)	105.4(4); −13.7(4)	6.017(5)	9.3(2)	167(3)
11	2.18(2)	35.9(2); −120.5(1)	−92.5(2); 18.0(2)	5.885(2)	4.5(8)	166(2)
32	1.98	−37.9(4); 122.8(3)	90.7(4); 21.7(4)	5.49^c	2.2	152
II β-turn (ideal)	1.8−2.5	−60; 120	80; 0	<7	0	160
II′ β-turn (ideal)	1.8−2.5	60; −120	−80; 0	<7	0	160

^{a} Two symmetry-independent molecules in the asymmetric unit. ^{b} Pseudodihedral angle formed by the four Cα atoms (or equivalents) of the peptide model. ^{c} The value corresponds to the $C\alpha_{(i)}{\cdots}H^ZN_{(i+3)}$ distance.

Supporting Information). To our delight (Figure 5), in each case, intramolecular hydrogen bonds were formed between the Aib or glycinamide $HN_{(i+3)}$ amide donors and the Boc or Pro C=$O_{(i)}$ oxygen atom acceptors, thereby creating a β-turn within the molecule which has a graph set[32] motif of S(10).

A more detailed analysis of the structural data, Table 2, revealed the presence of well defined β-turned conformations of type-II for **6** and **32** and of type-II′ for **11**, depending upon the configuration of the C_3 stereocenter at the respective β-lactam rings. In addition to the typical $_{(i)}C{=}O{\cdots}HN_{(i+3)}$ intramolecular hydrogen bonds, all of the four structural criteria[3] used to define canonical type-II β-turns are clearly fulfilled by the three peptidomimetics, suggesting that conformational behavior observed previously for model **6** could be extended to a variety of α-substituted α-amino-β-lactam peptides. Furthermore, the hydrogen bond directionality defined by the $_{(i)}O{\cdots}H{-}N_{(i+3)}$ angles is almost ideal in all instances.

Slight dihedral angle distortions of about 15−20° for the $\phi_{(i+1)}$, $\phi_{(i+2)}$, and $\psi_{(i+2)}$ angles with respect to native ideal values is also observed for **11** and **32**, whereas the rigid $\psi_{(i+1)}$ angle remains, as expected, constant and very close to the ideal 120° value. At the origin of this difference is the coplanar spatial arrangement of the $N_{(i+1)}$, $C\alpha_{(i+1)}$, $N_{(i+2)}$, and $C\alpha_{(i+2)}$ atoms, forced by the central β-lactam ring. This particular characteristic of α-substituted α-amino-β-lactam peptides seems to favor the formation of perfectly parallel peptide branches at the (i) and $(i+3)$ termini, as judged by the systematically small values of the pseudodihedral angle δ, and anticipates the use of these peptidomimetics, for instance, as promising antiparallel pleated β-sheet nucleators.[33]

Type II′ β-turned conformation of the model **11** (anti-α,β-dialkyl substituted at the β-lactam ring) is worth mentioning since, owing to the steric congestion caused by the isobutyl group, the −(β-lactam)-(gly)− segment in this compound was expected to display a markedly less betagenic behavior than models **6** or **10**. Nevertheless, the isobutyl group at the β-lactam ring C_4 position, the bulky $Aib_{(i+3)}$ residue, and the $Boc_{(i)}NH$ group are arranged on the same side of the plane defined by the four atoms of the β-lactam ring. Finally, the melanostatin Boc derivative **32** also displays a well-defined type II β-turn, including a short hydrogen bond (1.98 Å) between the proline C=$O_{(i)}$ oxygen atom and the glycine $H^EN_{(i+3)}$ hydrogen atom, similar to that in the previously reported crystal structure melanostatin hemihydrate (2.15 Å).[34]

Despite these promising results, it is well-known that solid-state secondary conformation of peptidomimetics is often conditioned by "lattice effects"[35] involving significant intermolecular hydrogen-bonding that, indeed, was clearly observed in our molecules.[36] Therefore, extension of the conclusions outlined above to biologically meaningful media necessitated assessment of the stability of the observed β-turns in highly coordinating solvent solutions. Although water was considered first, finally DMSO solvent was chosen for practical reasons (model compounds **6**, **8**, **9**, **10**, and **11** were insoluble in water) and also because the only NMR conformational study described for melanostatin **12** in solution was conducted in this solvent.[37]

Molecular Dynamics Simulations. MD simulations were carried out in a DMSO box at 300 K and 1 atm using the AMBER 6 force field (see the Experimental Section for details).

(32) For a detailed information on graph set definitions, see: Bernstein, J.; Davis, R. E.; Shimoni, L.; Chang, N.-L. *Angew. Chem., Int. Ed. Engl.* **1995**, *34*, 1555−1573.
(33) Nowick, J. S.; Smith, E. M.; Pairish, M. *Chem. Soc. Rev.* **1996**, 401−415.

(34) Reed, L. L.; Johnson, P. L. *J. Am. Chem. Soc.* **1973**, *95*, 7523.
(35) Steiner, T. *Angew. Chem., Int. Ed.* **2002**, *41*, 48−76.
(36) For details on intermolecular hydrogen bonding patterns of compounds **11** and **32**, see the Supporting Information.
(37) Higashijima, T.; Tasumi, M.; Miyazawa, T.; Miyoshi, M. *Eur. J. Biochem.* **1978**, *89*, 543−556.
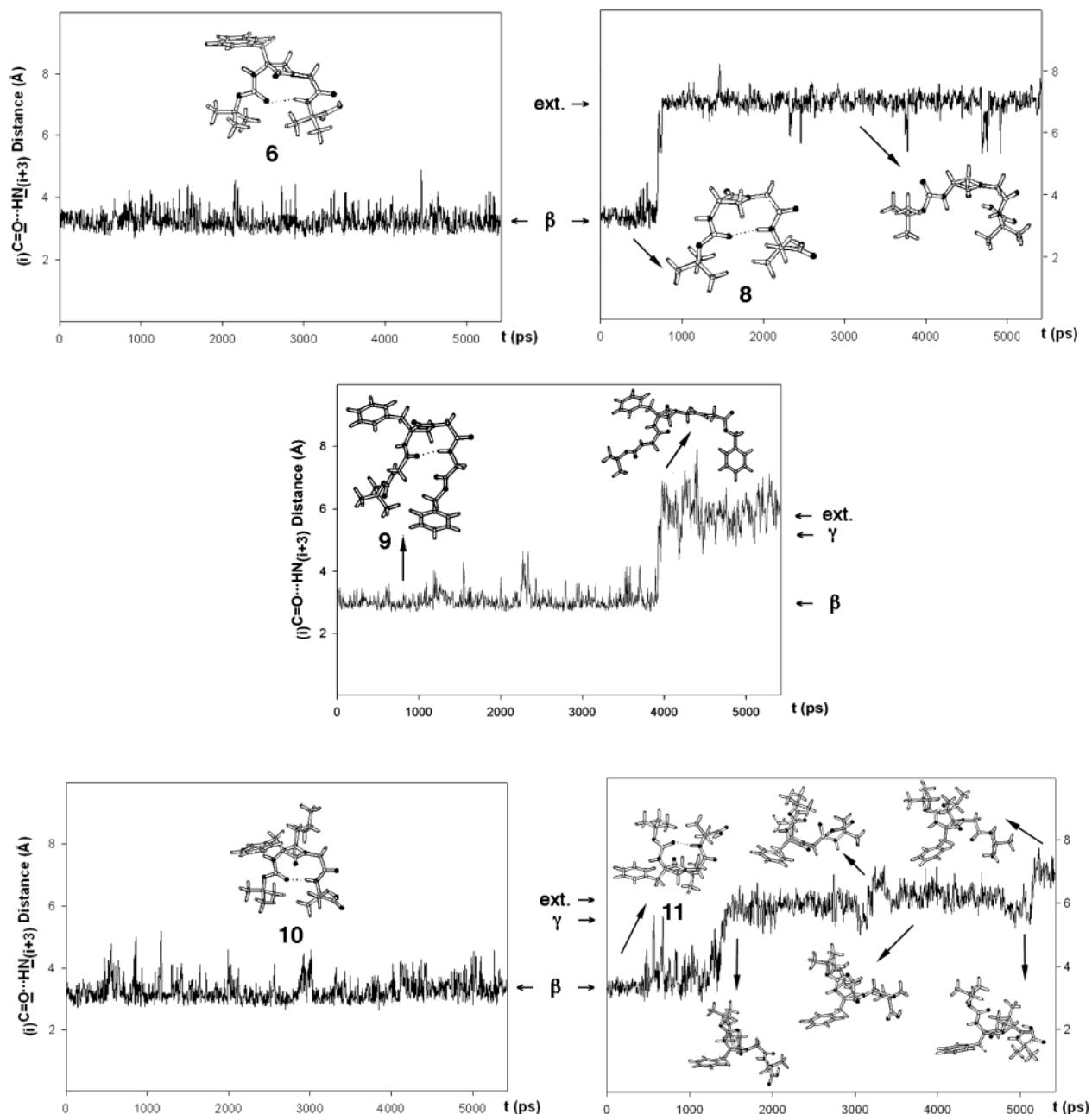
Figure 6. Values of the $_{(i)}C{=}O{\cdots}HN_{(i+3)}$ inter-residual hydrogen bond distances (Å) from the MD 5 ns trajectories of β-lactam model compounds **6**, **8**, **9**, **10**, and **11** calculated in DMSO solution.

The peptidomimetic β-lactam molecules **6**, **8**, **9**, **10**, **11**, and **13** were model-built using the bond lengths and angles taken from the crystal structures of compounds **6**, **11**, and **23**. The melanostatin **12** model was generated similarly from the reported crystal structure,[34] and the prolyl residue was uncharged. Type-II β-turn motif (type-II′ β-turn motif for compounds **8** and **11**) was reproduced, the restraint was removed thereafter, and the system coordinates were collected every picosecond for a 5 ns trajectory. The adoption of β-turn, γ-turn, or extended conformations around the $-(i{+}1){-}(i{+}2)-$ segment was assumed for average $_{(i)}C{=}O{\cdots}H{-}N_{(i+3)}$ distances of 3.2 ± 0.3 Å, 5.5 ± 0.3 Å, and >6.0 Å, respectively. The relevant results are shown in Figure 6.

Whereas the β-turn pattern remains stable over the 5ns trajectory of the MD simulation for mimetics **6** and **10**, analysis of the trajectories of compounds **8**, and especially **11**, reveals a great conformational heterogeneity. Peptide **6** only shows one conformation corresponding to a β-turn motif which fits reasonably well with the structural parameters of a slightly deformed type II β-turn, while compound **10** exhibits two deformed type II β-turns along the trajectory of the MD simulation. Values of β-turn dihedral angles are shown in Table 4 (see below). On the other hand, the comparatively lower stability of the β-lactam peptide model **9** with respect to **6** around the $-(\beta\text{-}Lactam){-}(Gly){-}$ fragment partially shaded our initial assumption concerning the stability of the β-turn motif in the absence of bulky Boc- and quaternary Aib residues at the N- and C− terminal positions.

Compound **11** quickly abandoned the type-II β-turn conformation and visited several extended and a few γ-turned forms, which was in contrast with the unique type-II′ conformation that was found in the solid state. This effect can be attributed
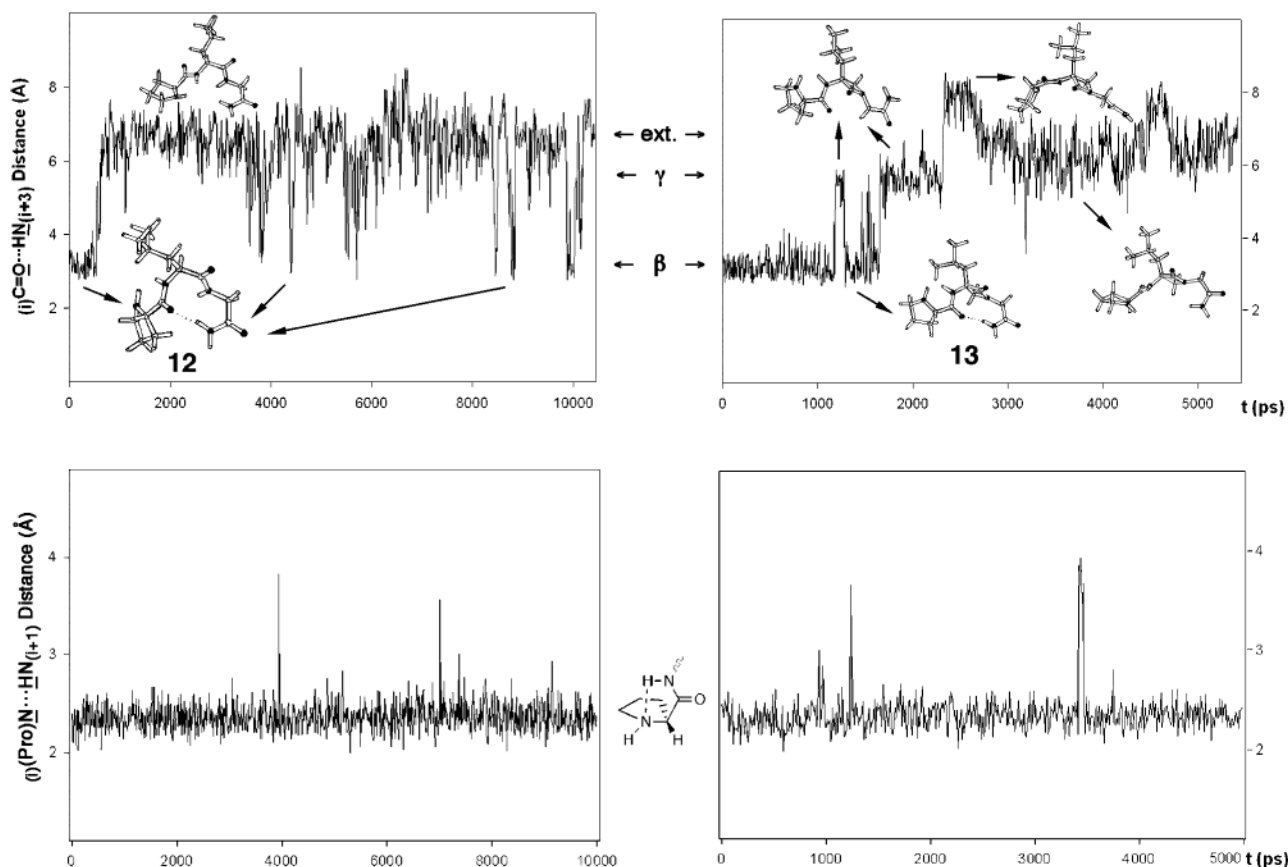
Figure 7. MD trajectories of melanostatin (PLG) **12** (10 ns, left) and β-lactam peptidomimetic **13** (5 ns, right) calculated in DMSO solution. Upper case: the $_{(i)}C{=}O{\cdots}HN_{(i+3)}$ inter-residual hydrogen bond distances. Lower case: the $_{(i)}$(proline)$N{\cdots}H$NCO$_{(i+1)}$ γ-turn distances.

most likely to the destabilizing effect of the DMSO solvent. A similar trend was observed for compound **8** as soon as the hydrogen-bonding distance restraint was removed, resulting in a remarkably homogeneous extended conformation. However, in this case the long $_{(i)}C{=}O{\cdots}H$-$N_{(i+3)}$ distances arose from the 180° rotation of the BocHN group around the $\phi_{(i+1)}$ dihedral angle and not from the relative disposition of the Gly-Aib branch with respect to the β-lactam ring. A comparison of the behavior of compound pairs **6/8** and **10/11** reveals the paramount importance of the presence of an alkyl substituent at the C_3 position as well as the relative syn/anti disposition of the substituents of the β-lactam ring in controlling β-turn stability, even in DMSO solution.

We also applied our MD protocol in DMSO to melanostatin **12** and the β-lactam peptidomimetic **13**. As the involvement of a five-atom loop, stabilized by a hydrogen bond between the Pro amine nitrogen and the Leu amide NH proton, has been suggested to explain the bioactivity of natural PLG amide **12**,[38] we monitored both the $_{(i)}C{=}O{\cdots}HN_{(i+3)}$ and the $_{(i)}$(Pro)$N{\cdots}HN_{(i+1)}$ distances along the trajectories of **12** and **13** (Figure 7). As can be inferred from these data, the β-turn for melanostatin is very unstable in DMSO and coexists with several extended conformations of the peptide. This behavior agrees with previously reported observations showing that unprotonated Pro-Leu-Gly-NH$_2$ is not rigid in DMSO solution.[37]

The MD conformational analysis of derivative **13** led to the identification of several conformations, apart from the moder-

ately populated type-II β-turn structure (average $_{(i)}C{=}O{\cdots}HN_{(i+3)}$ distance of 3.12 Å). Two of these conformations correspond to the intramolecular bridge between the terminal glycinamide $H^EN_{(i+3)}$ proton and the β-lactam $N_{(i+1)}$ nitrogen, giving rise to two possible five-membered rings: the first by the "upper" *re* face of the β-lactam, and the second by the "lower" *si* face. Finally, the high stability of the C_5 loop around the Pro residue was confirmed along all the trajectories of **12** and **13**, showing average $_{(i)}$(Pro)$N{\cdots}HN_{(i+1)}$ distances of 2.36 Å and constraining the (Pro) $\psi_{(i)}$ dihedral angle close to 0°.

NMR Conformational Analysis in Solution. The study of peptidomimetic models **6**, **8**, **9**, **10**, **11**, and **13** was conducted in DMSO-d_6, primarily by the temperature coefficient analysis and short-range NOE inspection to identify intramolecular hydrogen bonding and then using the procedure of Seebach and van Gusteren,[39] consisting of a cluster analysis of combined experimental (NMR-500 MHz) and simulated annealing data. Spin system identification (see Figure 8) and assignment of individual resonances were carried out using a combination of ^{1}H, DQF-COSY, and NOESY spectra, according to the standard procedures.[40] Single sets of signals were observed for all β-lactam pseudopeptides at 300 K under measurement conditions.

The involvement of the NH$_{(i+3)}$ amide protons in intramolecular hydrogen bonding (Table 3) was first estimated from

(38) Valle, G.; Crisma, M.; Toniolo, C.; Yu, K.-L.; Johnson, R. L. *Int. J. Peptide Protein Res.* **1989**, *33*, 181−187.

(39) Daura, X.; Gademann, K.; Schäfer, H.; Jaun, B.; Seebach, D.; van Gunsteren, W. F. *J. Am. Chem. Soc.* **2001**, *123*, 2393−2404.

(40) (a) Kessler, H.; Schmitt, W. In *Encyclopedia of Nuclear Magnetic Resonance*; Grant, D. M., Harris, R. K., Eds.; J. Wiley & Sons: New York, 1995. (b) Güntert, P. *Quart. Rev. Biophys.* **1998**, *31*, 142−237.
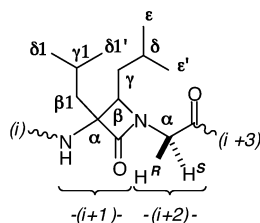
Figure 8. Definition of the substituent atoms of a general $-(\beta$-lactam)-(Gly)$-$ segment used for the conformational study.

Table 3. Temperature Coefficients (ppb/K) of the Amide NH Protons Measured for β-Lactam Peptidomimetics **6**–**13** (DMSO$_{D6}$, 500 MHz) at 5 K Intervals between 300 and 325 K[a]

compd	H$-$N$_{(i)}$	H$-$N$_{(i+1)}$	H$-$N$_{(i+3)}$
6		-8.3 (2.21)	-2.3 (0.03)
8		-5.1 $(-)^b$	-4.9 $(-)^b$
9	-6.4 (1.83)	-5.9 (1.50)	-4.2 (0.25)
10		-10.0 (2.51)	-2.9 (0.08)
11		-8.9 (2.48)	-3.1 (0.03)
13		-2.6 $(-)^b$	-3.9 H^{E}N $(-)^b$; ^{b} -6.5 H^{Z}N $(-)^b$

^{a} Data in parentheses correspond to chemical shift differences (ppm) caused by the solvent effect (δ DMSO-d_6 $-$ δ CDCl$_3$) at 300 K. ^{b} Compound insoluble in CDCl$_3$ solvent.

temperature coefficients (DMSO-d_6) and from chemical shift differences in coordinating (DMSO-d_6) and noncoordinating (CDCl$_3$) solvents. All data were recorded at 10$-$15 mM concentrations. No chemical shift or line-width variation was observed, compared with a 10-fold dilution, which confirmed the absence of any noticeable intermolecular aggregation.

Significant small temperature coefficients (<3 ppb/K)[41] and chemical shifts changes were found for the NH$_{(i+3)}$ protons of compounds **6**, **10**, and **11**, thus confirming their participation in intramolecular hydrogen bonding. The tetrapeptide analogue **9** showed slightly larger values, whereas for the α-unsubstituted β-lactam pseudopeptide **8**, the NH$_{(i+3)}$ proton could not be considered to form a stable intramolecular hydrogen bond. Interestingly, the temperature coefficients of the glycinamide H^{E}N$_{(i+3)}$ and H^{Z}N$_{(i+3)}$ protons differed for the melanostatin analogue **13** but not for natural melanostatin **12** (H^{E}N$_{(i+3)}$: -5.2 ppb/K; H^{Z}N$_{(i+3)}$: -5.5 ppb/K).[37] The coalescence temperature was also found to be 30° higher for **13** (375 K) than for **12** (345 K), suggesting a relative stabilization of the hydrogen-bonded structure caused by the presence of the β-lactam ring. Finally, the low-temperature coefficients measured for HN$_{(i+1)}$ amide in **13** agreed fully with the C$_5$ loop structure calculated by MD simulation around the Pro$_{(i)}$ residue.

Inspection of the NOESY cross-peak signals from the amide HN$_{(i+3)}$ and β-lactam ring H$\beta1_{(i+1)}$ protons (Figure 9) proved to be particularly informative as a qualitative indication of the acceptors involved in the intramolecular hydrogen-bonded conformations, since the diastereotopic protons H$^R\beta_{(i+1)}$ and H$^S\beta_{(i+1)}$ were easily distinguished from each other by the $^3J(CH\alpha-CH\beta)$ coupling constants in **8** or using selective NOESY experiments between the H$^R\beta_{(i+1)}$ and the benzyl or isobutyl H$\beta1_{(i+1)}$ protons in models **6**, **9** and **13**. This allowed a tentative location of the $-(Gly)-(i+3)$ branch in the lower or upper plane of the β-lactam ring and gave an important indication to establish the presence of β-turned or extended/γ-turned conformations, respectively.[42] Both **6** and **9** showed

strong NOEs of the respective HN$_{(i+3)}$ amides of the Aib and GlyOBn residues with the β-lactam H$^S\beta_{(i+1)}$ protons, but not with H$^R\beta_{(i+1)}$. In sharp contrast with this behavior, the HN$_{(i+3)}$ amide of **8** displayed interactions with both H$\beta_{(i+1)}$ protons which, in combination with the high-temperature coefficients measured above, suggested an equilibrium between several extended conformations. Finally, the PLG analogue **13** also showed strong NOE signals of both glycinamide HN$_{(i+3)}$ protons exclusively with the β-lactam H$^S\beta_{(i+1)}$ protons, providing evidence of the presence of a β-turned conformation.

In the case of syn-/anti-α,β-disubstituted tetrapeptide models **10** and **11** (see Figure 10) only one H$\beta_{(i+1)}$ proton was available for observation and a supplementary region of the spectrum involving isobutyl group protons ($\sim0.7-2$ ppm) was examined for evidence of close interproton interactions of HN$_{(i+3)}$ with the alkyl groups placed in the upper face of the β-lactam ring plane. Again, peptide model **10** showed a strong bias for a β-turned conformation, as judged by the HN$_{(i+3)}$/H$\beta_{(i+1)}$ NOE signal and the absence of any cross-peak between HN$_{(i+3)}$ and isobutyl or benzyl protons. On the other hand, *anti*-peptide **11** presented no NOE cross-peaks between HN$_{(i+3)}$ and H$\beta_{(i+1)}$ and only a weak interaction of HN$_{(i+3)}$ with the isobutyl methylene protons, which was also consistent with a β-turn conformation. This observation partially refuted the extended or γ-turned conformations provided by MD calculations and agreed better with the solid-state structure derived from X-ray crystallographic analysis.

After qualitative identification of folded start conformations, 100 structures were generated for each β-lactam peptidomimetic model **6**, **8**, **9**, **10**, **11**, and **13** using the X-PLOR[43] program, and only acceptable conformers presenting no violations of NOESY-derived interprotonic distance restraints were analyzed. Clusters were created applying the same $_{(i)}$C$=O\cdots$H$N_{(i+3)}$ intervals used for MD analysis (see above), and the values of the main structural parameters resulting from each cluster were analyzed (Table 4, Figure 11).

In excellent agreement with the X-ray crystallography and MD data, each peptide model **6** and **10** presented only one very populated cluster mimicking a canonical type-II β-turn around the $-(\beta$-lactam)-(Gly)$-$ segment. Compounds **11** and **9** also reproduced correctly folded β-turns, but they enjoyed an excess of conformational freedom. In both instances, an appreciable distortion of the pseudodihedral angle δ (25$-$35°) was observed, which could be at the origin of the mobility observed during MD trajectories. Nonetheless, it is worth mentioning that, neither the *anti*-α,β-dialkyl substitution pattern of the β-lactam ring in **11**, nor the presence of fully flexible glycine residues at the N- and C-terminal positions of **9** sufficed to destabilize these β-lactam peptide models to extended conformations in DMSO.

On the other hand, the α-nonalkylated pseudopeptide **8** presented, apart from the starting type II β-turn conformation cluster (**8-A**), a second extended cluster (**8-B**) clearly defined by the rotation of the BocHN group around the $\phi_{(i+1)}$ dihedral angle. Finally, melanostatin β-lactam analogue **13** is also distributed into two similarly populated clusters (**13-A** and **13-**

(41) Kessler, H. *Angew. Chem., Int. Ed. Engl.* **1982**, *21*, 512$-$523.

(42) The formation of a seven-membered γ-turn structure in β-lactam pseudopeptides through hydrogen-bonding of HN$_{(i+3)}$ amide to β-lactam C$=$O$_{(i+1)}$ oxygen has previously been suggested by our group, see ref 14(b). An alternative five-membered γ-turn from HN$_{(i+3)}$ amide to β-lactam N$_{(i+1)}$ has also been calculated; see ref 16a.
(43) Schwieters, C. D.; Kuszewski, J.; Tjandra, N.; Clore, G. M. *J. Magn. Reson.* **2003**, *160*, 66$-$74.
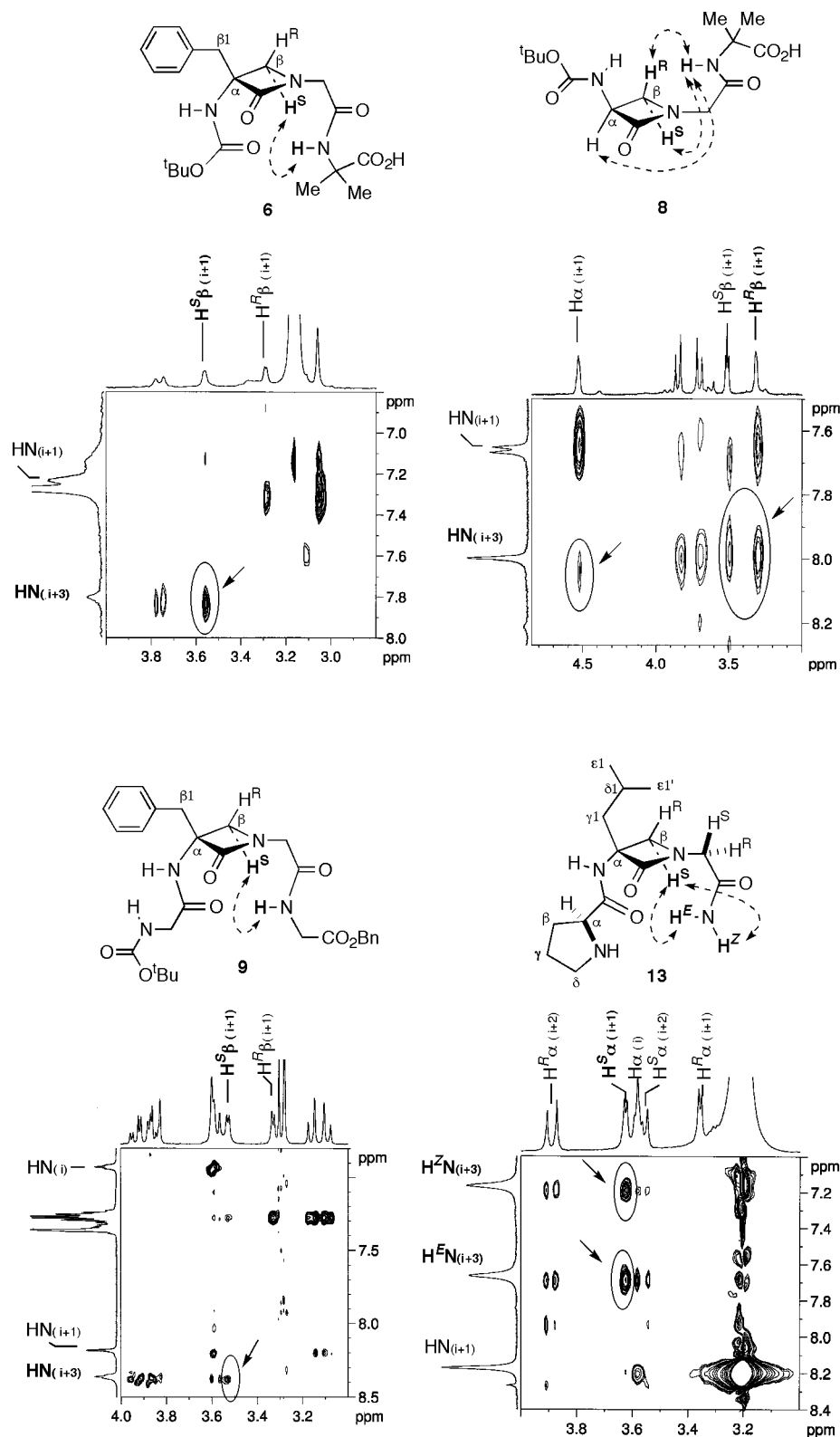
Figure 9. Selected expansions of NOESY spectra (500 MHz) showing the amide NH and β-lactam Hβ regions of **6**, **8**, **9**, and **13** in DMSO-d_6 (10−15 mM), 400 ms mixing time, recorded at 300 K. Marked cross-peaks indicate a β-turn or extended conformations.

B) having, respectively, the type-II and extended conformations. Apparently, the $\phi_{(i+1)}$ dihedral angle blocking exerted by the isobutyl group in this case is less effective than α-benzyl blocking (see pseudopeptides **6**, **9**, **10**, or **11**) and allows a partial conformational freedom, as anticipated by MD calculations.

Biological Evaluation of Melanostatin (PLG) β-Lactam Analogue 13. Several studies have shown that PLG and its peptidomimetic analogues render the Gi-protein coupled dopamine D_2-like receptors more responsive to agonists by maintaining the high-affinity binding state of the receptor,[44] albeit the exact
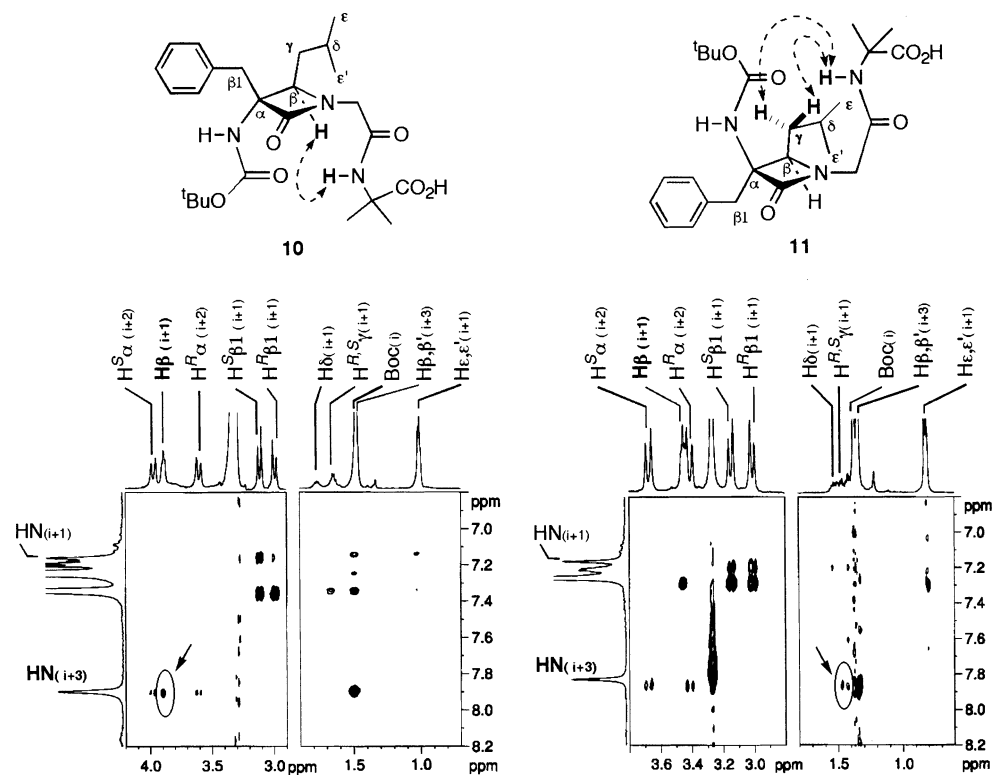
Figure 10. Selected expansions of NOESY (500 MHz) experiments of **10** and **11** in DMSO-d_6 (8.5 and 12 mM), 400 ms mixing time, recorded at 300 K. β-Lactam H$\beta_{(i+1)}$, glycine H$\alpha_{(i+2)}$ (top left) and isobutyl proton regions (top right) are compared to NH amide region (left). Marked cross-peaks indicate a β-turn conformation.

Table 4. Averaged Structural Parameters of the Conformation Clusters of β-Lactam Peptidomimetic Models **6−13** Obtained with X-PLOR from NOESY-Restrained NMR Data

cluster (n)[a]	type	$\langle_{(i)}C{=}O{\cdots}HN_{(i+3)}\rangle^b$ (Å)	$\langle(\phi;\psi)_{(i+1)}\rangle^c$ (deg)	$\langle(\phi;\psi)_{(i+2)}\rangle^c$ (deg)	$\langle C\alpha_{(1)}{\cdots}C\alpha_{(1+3)}\rangle$ (Å)	δ^d (deg)
6-A (83)	β-II turn	2.9 (2.1)	−27; 114 (−20; 110)	109; −40 (55; 25)	5.5	5.7
8-A (58)	β-II′ turn	3.1 (2.5)	21; −118 (25; −110)	−96; 48 (−75; 0)	5.7	3.7
8-B (42)	extended	6.3 (5.8)	177; −118	−96; 48	7.2	21
9-A (58)	β turn[e]	3.6 (3.5)	−30; 116	82; 70	6.0	25
9-B (37)	β turn[e]	4.1 (3.8)	28; 115	86; 82	6.5	35
10-A (89)	β-II turn	3.1 (2.5)	−36; 113 (−20; 110)	56; 29 (50; 40)	5.3	−17
11-A (33)	β-II′ turn	3.2 (2.4)	30; −117 (20; −120)	−53; 34 (110; −40)	5.9	34
13-A (43)	β-II turn	3.0 (2.5)	−49; 120 (−47; 123)	111; −39 (92; 22)	− −[f]	24
13-B (40)	extended	5.9 (4.9)	−145; 120	105; −37	− −[f]	7

[a] Number of structures with no violations of NOESY interprotonic distance restraints per cluster from 100 structures generated. [b] Values in parentheses indicate average $_{(i)}C{=}O{\cdots}HN_{(i+3)}$ distance. [c] Values in parentheses indicate average $-(i+1)-(i+2)-$ dihedral angles calculated from MD simulations for the whole trajectory of each compound. Ideal dihedral angles: type β-II: $(\phi;\psi)_{(i+1)} = -60$; 120; $(\phi;\psi)_{(i+2)} = 80$; 0, type β-II′ $(\phi;\psi)_{(i+1)} = 60$; −120; $(\phi;\psi)_{(i+2)} = -80$; 0. [d] Pseudodihedral angle formed by the four Cα atoms (or equivalents) of the peptide model. [e] Noncanonical distorted β-turns. [f] Hydrogen atom placed at the C$\alpha_{(i+3)}$ position.

nature of the molecular interactions of PLG in such a process remains obscure. All of the research conducted thus far to quantify the bioactivity of PLG has focused primarily on the behavioral inspection of whole animal models and on radioligand competitive binding assays of receptors obtained from tissue homogenates. However, as the mechanism of action of PLG may likely involve intraneuronal enzymes,[45] direct competitive binding assays on integral neurons should be highly desirable to provide information more directly assignable to real living systems.

To test the relative activity of β-lactam analogue **13** versus natural PLG **12** as a dopamine D$_2$ receptor modulator, we

conducted for the first time radioligand competitive binding assays[46] on cultured integer neuron cells[47] from rat cerebral cortex. The experiments involved the blocking of D$_2$ receptors in neurons with the specific tritiated antagonist [^{3}H]spiroperidol, followed by addition of increasing amounts of agonist N-propylnorapomorphine (NPA), either in the absence (control) or in the presence of fixed concentrations of PLG **12** and its β-lactam analogue **13**. Representative competitive binding

(44) The signal transduction mechanism triggered by dopamine in D$_2$ receptors leads ultimately to an intraneuronal cyclic adenosyl monophosphate (cAMP) concentration reduction with the intermediacy of Gi proteins of "high" and "low" affinity corresponding, respectively, to di- and triphosphorilated species; see: Costain, W. J.; Gupta, S. K.; Johnson, R. L.; Mishra, R. K. *G Protein Methods Protocols* **1997**, *31*, 119−138.

(45) Two putative mechanisms have been proposed. First, the PLG-mediated allosteric stabilization of the dopamine/D$_2$ receptor/Gi protein ternary complex at the membrane and, second, the intraneuronal stimulation of guanosine triphosphatase enzyme (GTPase) and simultaneous inhibition of adenosyl cyclase enzyme (AC), see: Mishra, R. K.; Makman, M. H.; Costain, W. J.; Nair, V. D.; Johnson, R. L. *Neurosci. Lett.* **1999**, *269*, 21−24.

(46) Baures, P. A.; Ojala, W. H.; Costain, W. J.; Ott, M. C.; Pradhan, A.; Gleason, W. B.; Mishra, R. K.; Johnson, R. L. *J. Med. Chem.* **1997**, *40*, 3594−3600.

(47) Abele, A. E.; Scholz, K. P.; Scholz, W. K.; Miller, R. *Neuron* **1990**, *2*, 413−419.
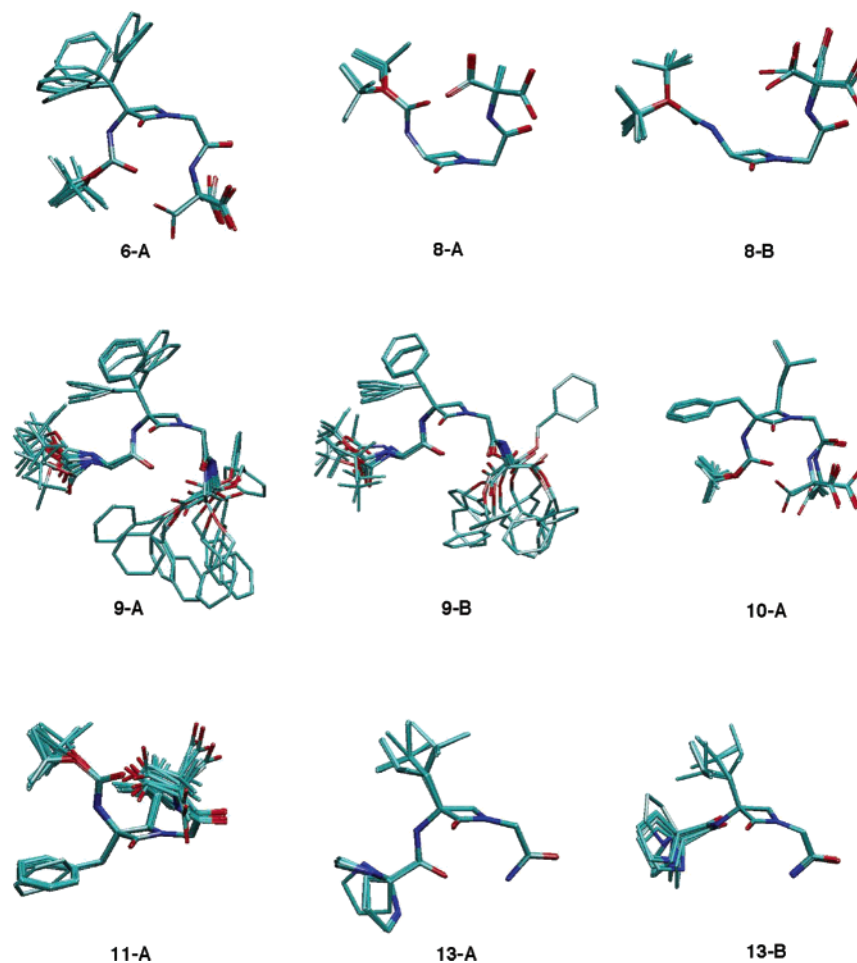
Figure 11. Views of the backbone superposition of 10 structures of lowest energy with NOESY distance restraints derived from NMR data for conformational clusters **6-A**−**13-B**. Calculations performed in vacuo with X-PLOR.
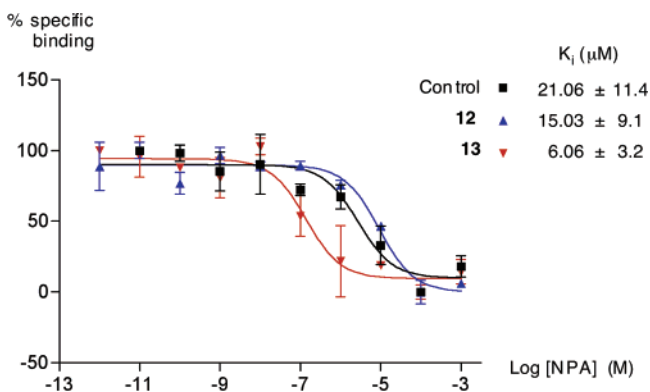

Figure 12. Representative competition curve of [³H]spiroperidol/*N*-propylnorapomorphine (NPA) in cultured neurons from rat cerebral cortex without treatment (control) and treated with PLG **12** (1 μM) or PLG peptidomimetic **13** (1 μM). The concentration of [³H]spiroperidol in the assay was 0.5 nM; previously determined K_d was 0.99 nM. Inhibiton constant (K_i) of agonist, calculated for the [³H]spiroperidol binding using expressed as mean ± SEM from four separate experiments done in triplicate. Nonspecific binding was determined in parallel assays in the presence of 1 μM (+)-butaclamol.

curves, see Figure 12, indicated that **13** slightly reduces the dissociation constant of dopamine D_2 receptors for NPA with respect to PLG **12** at a micromolar concentration range. Despite the low accuracy of the measurements, which not allow one to distinguish between high- and low-affinity binding constants, the full retention of bioactivity on living neurons observed for

13 with respect to PLG **12** suggests that the structural variation arising from the replacement of $C\alpha H_{(i+1)}$ and $HN_{(i+2)}$ protons by a β-lactam methylene group does not hinder the maintenance of a similar recognition pattern by D_2 receptors.

Conclusions. A simplified peptidomimetic design based on the concept of separation of constraint and recognition elements has been developed to prepare short pseudopeptides containing enantiopure α-substituted α-amino-β-lactam fragments that mimic very stable β-turns of type II or type II′ with highly predictable stereostructural properties. X-ray crystallography in the solid state and MD or NMR conformational studies in dimethyl sulfoxide solutions have shown that the α-alkyl-α-amino substitution pattern of β-lactam rings placed as −(i+1)− residues in tetrapeptide models is essential to fold the peptidomimetic to a stable β-turned conformation. syn-α,β-Disubstitution seems not to provide additional stabilizaton and even anti-α,β-disubstitution is compatible with β-turn formation in polar solvents. The nature of the N- and C-terminal residues in tetrapeptide models has little effect, albeit observable, on the betagenic ability of the central −(β-lactam)-(Gly)− segment since even models flanked by two glycine units afford rough but correctly folded β-turned structures.

Finally, conservation of the recognition requirements of the binding pocket in the receptor for PLG neuropeptide β-lactam analogue **13**, despite the incorporation of a methylene bridging in native PLG **12**, seems to confirm the viability of a design

separating constraint and recognition groups. Work to illustrate the application of these novel β-lactam peptidomimetics to the ligand-based β-turned agonists for G-protein-coupled receptors is in progress in our laboratory.

Experimental Section

General Methods. All reactions were carried out under an atmosphere of nitrogen in oven- or flame-dried glassware with magnetic stirring. Solvents were distilled prior to use. Tetrahydrofuran (THF) was distilled from sodium metal/benzophenone ketyl. Acetonitrile (CH$_3$-CN) and dichloromethane (CH$_2$Cl$_2$) were distilled from calcium hydride. Methanol (MeOH) was dried over magnesium metal and iodine. DMF was purified by distillation on barium oxide. Purification of reaction products was carried out by flash chromatography using silica gel 60 (230−400 mesh, from Merck 60F PF254). Analytical thin-layer chromatography was performed on 0.25 mm silica gel 60-F plates. Visualization was accomplished with UV light and phosphomolybdic acid−ammonium cerium(IV) nitratesulfuric acid−water reagent, followed by heating. Melting points were measured with a Büchi SMP-20 melting point apparatus and are uncorrected. Infrared spectra were recorded on a Shimadzu IR-435 spectrophotometer. ^{1}H NMR and ^{13}C NMR spectra were recorded on a Bruker Avance DPX300 and Bruker Avance500 spectrometers and are reported as δ values (ppm) relative to residual CHCl$_3$ δ_H (7.26 ppm) and CDCl$_3$ δ_C (77.16 ppm) as internal standards, respectively. Combustion analyses were performed on a Leco CHNS-932 elemental analyzer. Analytical high-performance liquid chromatography (HPLC) was performed on a Hewlett-Packard 1050 chromatograph equipped with a diode array UV detector, using the analitycal columns (25 cm, phase Lichrosorb-Si60) and (25 cm, phase Chiralcel OD) with flow rates of 1 and 0.5 mL/min, respectively, and on preparative-scale columns (25 × 2.5 cm, phase Lichrosorb-Si60). Optical rotations were measured at 25 ± 0.2 °C in methylene chloride unless otherwise stated. Mass spectra were obtained on a Finnigan GCQ mass spectrometer (70 eV) using GC−MS coupling (column: fused silica gel, 15 m, 0.25 mm, 0.25 nm phase SPB-5). Compounds **4**,[22a] **17**,[26] **24**,[26] and **25**[26] were prepared according to described procedures.

General Procedure for the Carboxymethylation of 3-*tert*-Butoxycarbonylamino-NH-β-lactams. Synthesis of 15, 20, and 23. A solution of the corresponding NH-β-lactam (5 mmol) in dry MeCN (50 mL) was prepared under nitrogen in a flame-dried two-necked flask fitted with a septum and a thermometer. The temperature was warmed to 50 °C using a water bath, Cs$_2$CO$_3$ (6.0 mmol, 1.96 g) and benzyl iodoacetate (7.5 mmol, 1.39 g) were added, and the mixture was stirred for 3 h at the same temperature. Water (50 mL) and EtOAc (100 mL) were added to the mixture, the organic layer was separated, and the aqueous phase was extracted with EtOAc (30 mL × 3). The combined organic solutions were dried (MgSO$_4$) and evaporated under reduced pressure. The intermediate *N*-[(benzyloxycarbonyl)methyl]-β-lactam was purified by column chromatography (silica gel; eluant: EtOAc/hexanes). This product was dissolved in dried EtOAc (30 mL), 10%Pd/C (0.2 g) was added, and the suspension was stirred under hydrogen (1 atm) for 4−8 h. The reaction mixture was filtered through Celite, washed with EtOAc (30 mL × 2), and evaporated in vacuo to afford the pure product.

(*S*)-3-*tert*-Butoxycarbonylamino-1-carboxymethylazetidin-2-one (15). The general procedure was followed from (*S*)-3-*tert*-butoxycarbonylaminoazetidin-2-one (**14**) (5 mmol, 0.93 g); eluant EtOAc/hexanes 1:5, then 1:1. Intermediate benzyl ester: (*S*)-1-[(benzyloxycarbonyl) methyl]-3-*tert*-butoxycarbonylamino-azetidin-2-one. [α]$^{25}_D$ = −3.4 (*c* = 1.0, Cl$_2$CH$_2$). IR (cm^{-1}, KBr): 2976.6; 2928.4(NH); 1746.3; 1712.5 (CO). ^{1}H NMR (δ, ppm, CDCl$_3$): 7.37 (s, 5H, Ar); 5.17−5.14 (sb, 2H, C*H*$_2$Ph, N*H*Boc); 4.93 (s$_b$, 1H, C*H*NHBoc); 4.07 (s$_b$, 2H, C*H*$_2$CO$_2$Bn); 3.73 (t, 1H, *J* = 5.4 Hz, C*H*$_2$-β-lactam); 3.40 (dd, 1H, *J* = 2.6, 5.4 Hz, C*H*$_2$-β-lactam); 1.44 (s, 9H, C(CH$_3$)$_3$). ^{13}C NMR (δ, ppm, CDCl$_3$): 168.8; 168.1; 155.5; 135.6;

129.7; 129.4; 81.2; 69.1; 58.9; 50.7; 43.7; 28.9. Reaction time (hydrogenation): 8 h. Yield (overall): 0.49 g (40%).

(3*R*,4*R*)-3-Benzyl-3-*tert*-butoxycarbonylamino-1-carboxymethyl-4-isobutylazetidin-2-one (20). The general procedure was followed from (3*R*,4*R*)-3-benzyl-3-*tert*-butoxycarbonylamino-4-isobutyl azetidin-2-one (**19**) (5 mmol, 2.23 g); eluant EtOAc/hexanes 1:3. Intermediate benzyl ester: (3*R*,4*R*)-3-benzyl-1-(benzyloxycarbonyl methyl)-3-*tert*-butoxy carbonylamino-4-isobutyl-azetidin-2-one. [α]$^{25}_D$ = −11.79 (*c* = 0.48, Cl$_2$CH$_2$). IR (cm^{-1}, KBr): 3263 (NH); 1758.7; 1732.0; 1720.9 (C=O). MS *m/z* (int): 91 (44.2); 129 (26.0); 146 (100.0); 189 (20.7); 215 (7.6); 234 (18.6); 324 (11.1); ^{1}H NMR (δ, ppm, CDCl$_3$): 7.37−7.20 (m, 10H, Ar); 5.22 (d, 1H, *J* = 11.7 Hz, OC*H*$_2$Ph); 5.15 (d, 1H, *J* = 12.2 Hz, OC*H*$_2$Ph); 4.65 (s, 1H, N*H*Boc); 4.46 (d, 1H, *J* = 18.1 Hz, NHC*H*$_2$CO); 3.99 (t, 1H, *J* = 6.4 Hz, *H*C(^{i}Bu)); 3.69 (d, 1H, *J* = 18.1 Hz, NHC*H*$_2$CO); 3.37 (d, 1H, *J* = 13.7 Hz, C*H*$_2$Ph); 3.16 (d, 1H, *J* = 14.1 Hz, C*H*$_2$Ph); 1.55−1.49 (m, 1H, C*H*$_2$CH(CH$_3$)$_2$); 1.47−1.36 (m, 2H, C*H*$_2$CH(CH$_3$)$_2$); 1.42 (s, 9H, OCOC(C*H*$_3$)$_3$); 0.83 (d, 3H, *J* = 6.4 Hz, CH$_2$CH(C*H*$_3$)$_2$); 0.81 (d, 3H, *J* = 6.4 Hz, CH$_2$CH(C*H*$_3$)$_2$). ^{13}C NMR (δ, ppm, CDCl$_3$): 168.9; 168.1; 154.3; 135.2; 134.9; 129.9; 128.7; 128.6; 127.3; 80.1; 70.2; 67.3; 63.1; 41.6; 40.3; 37.1; 28.2; 25.7; 23.0; 22.5. Reaction time (hydrogenation): 4 h. Yield (overall): 1.69 g (87%).

(3*S*,4*R*)-3-Benzyl-3-*tert*-butoxycarbonylamino-1-carboxymethyl-4-isobutylazetidin-2-one (23): The general procedure was followed from (3*R*,4*R*)-3-benzyl-3-*tert*-butoxycarbonylamino-4-isobutyl azetidin-2-one (**22**) (5 mmol, 2.23 g); eluant EtOAc/hexanes 1:10 then 1:5. Intermediate benzyl ester: (3*S*,4*R*)-3-benzyl-1-(benzyloxycarbonyl-methyl)-3-*tert*-butoxycarbonylamino-4-isobutyl-azetidin-2-one. [α]$^{25}_D$ = +23.3 (*c* = 1.0, Cl$_2$CH$_2$). IR (cm^{-1}, KBr): 2946.0 (NH); 1761.1; 1751.3; 1748.3; 1707.8 (C=O). MS *m/z* (int): 91 (31.3); 129 (15.9); 146 (100); 189 (22.3); 324 (5.5). ^{1}H NMR (δ, ppm, CDCl$_3$): 7.41−7.30 (m, 10H, Ar); 5.23 (s, 2H, OC*H*$_2$Ph); 4.96 (s, 1H, NH); 4.13−4.11 (m, 3H, CC*H*; NC*H*$_2$CO); 3.34 (d, 1H, *J* = 13.4 Hz, C*H*$_2$Ph); 3.08 (d, 1H, *J* = 14.0 Hz, C*H*$_2$Ph); 1.75−1.60 (m, 3H, C*H*C*H*$_2$(CH$_3$)$_2$); 1.46 (s, 9H, Boc); 0.98 (d, 3H, *J* = 3.8 Hz, CH$_3$); 0.96 (d, 3H, *J* = 3.8 Hz, CH$_3$). ^{13}C NMR (δ, ppm, CDCl$_3$): 168.5; 168.0; 154.4; 135.4; 135.0; 130.4; 128.6; 128.5; 128.4; 128.2; 126.8; 79.9; 69.1; 67.3; 63.9; 42.4; 38.2; 35.2; 28.2; 25.9; 23.4; 21.8. Reaction time (hydrogenation): 4 h. Yield (overall): 1.60 g (82%).

General Procedure for Peptide Coupling of 3-*tert*-Butoxycarbonylamino-*N*-(carboxymethyl)-β-lactams with Benzyl 2-Aminoisobutyrate Tosylate (TsOH·AibOBn): Synthesis of 8, 10, and 11. To a solution of TsOH·AibOBn (3.0 mmol, 1.096 g) and NEt$_3$ (10.0 mmol, 1.39 mL) in dry CH$_2$Cl$_2$ (15 mL) cooled to 0 °C were added HOBt (2.0 mmol, 0.27 g) DMF (0.5 mL), the corresponding 3-*tert*-butoxycarbonylamino-*N*-(carboxymethyl)-β-lactam (2.0 mmol), and EDC·HCl (4.0 mmol, 0.767 g). The reaction mixture was stirred at 0 °C for 1 h, and then the bath was removed and the solution was stirred at room temperature overnight. CH$_2$Cl$_2$ (30 mL) was added, and the organic solution was successively washed with 0.1 M KHSO$_4$ (20 mL × 3; until neutral pH) and H$_2$O (20 mL × 2), dried (MgSO$_4$), and evaporated under reduced pressure. The intermediate benzyl ester was purified by column chromatography (silica gel; eluant: EtOAc/hexanes). This product was dissolved in dried EtOAc (10 mL), 10%Pd/C (0.10 g) was added, and the suspension was stirred under hydrogen (1 atm) for 4−24 h. The reaction mixture was filtered through Celite, washed with EtOAc (10 mL × 2), and evaporated in vacuo to afford the pure product.

(*S*)-1-(3-Aza-5-carboxy-4-methyl-2-oxopentyl)-3-*tert*-butoxycarbonylaminoazetidin-2-one (8). The general procedure was followed from (*S*)-3-*tert*-butoxycarbonylamino-1-carboxymethyl-azetidin-2-one (**15**) (2.0 mmol, 0.49 g); eluant EtOAc/hexanes 1:4. Intermediate benzyl ester: (*S*)-1-(3-aza-5-benzyloxycarbonyl-4-methyl-2-oxo-pentyl)-3-*tert*-butoxycarbonylaminoazetidin-2-one. IR (cm^{-1}, film NaCl): 3331 (NH); 2980; 2931; 1747; 1692 (CO); 1532. ^{1}H NMR (δ, ppm, CDCl$_3$): 7.62 (s, 1H, N*H*CMe$_2$); 7.27 (m, 5H, Ar); 5.28 (d, 1H, *J* = 7.6 Hz, N*H*Boc); 5.13 (d, 2H, *J* = 8.9 Hz, C*H*$_2$Ph); 5.08 (d, 2H, *J* = 8.9 Hz, C*H*$_2$Ph); 4.40 (d, 1H, *J* = 13.3 Hz, C*H*$_2$CONH); 4.34 (m, 1H, C*H*NHBoc); 3.59

(dd, 1H, J = 2.6, 5.6 Hz, CH_2 lactam); 3.40 (m, 1H, CH_2 lactam); 3.37 (d, 1H, J = 13.3 Hz, CH_2CONH); 1.53 (s, 3H, CH_3); 1.48 (s, 3H, CH_3); 1.36 (s, 9H, C(CH_3)$_3$). ^{13}C NMR (δ, ppm, CDCl$_3$): 167.5; 167.2; 155.6; 136.7; 129.1; 128.7; 81.7; 67.6; 59.4; 57.3; 48.1; 45.9; 28.9; 26.6; 25.2. Reaction time (hydrogenation): 24 h. Yield (overall): 0.612 g (93%).

(3R,4R)-1-(3-Aza-4-carboxy-4-methyl-2-oxopentyl)-3-benzyl-3-*tert*-butoxycarbonylamino-4-isobutylazetidin-2-one (10). The general procedure was followed from (3R,4R)-3-benzyl-3-*tert*-butoxycarbonyl-amino-1-carboxymethyl-4-isobutylazetidin-2-one (**20**) (2.0 mmol, 0.781 g); eluant EtOAc/hexanes 1:3. Intermediate benzyl ester: (3R,4R)-1-(3-aza-4-benzyloxycarbonyl-4-methyl-2-oxopentyl)-3-benzyl-3-*tert*-bu-toxiaminocarbonyl-4-isobutylazetidin-2-one. [α]$^{25}_D$ = +66.2 (c = 0.52, Cl$_2$CH$_2$). IR (cm^{-1}, KBr): 3322.5; 2950.0 (NH); 1763.9; 1744.0; 1691.4; 1678.9 (C=O); ^{1}H NMR (δ, ppm, CDCl$_3$): 7.83 (s, 1H, NHC=O); 7.39−7.28 (m, 10H, Ar); 5.17 (s, 2H, OCH_2Ph); 4.70 (s, 1H, NHBoc); 4.42 (d, 1H, J = 17.6 Hz, NCH_2C=O); 4.28 (t, 1H, J = 6.45 Hz, CH-^{i}Bu); 3.52 (d, 1H, J = 17.4 Hz, NCH_2C=O); 3.22 (d, 1H, J = 14.7 Hz, CH_2Ph); 2.94 (d, 1H, J = 14.8 Hz, CH_2Ph); 1.69−1.51 (m, 3H, CH_2CH(CH$_3$)$_2$); 1.58 (s, 3H, −NHC(CH_3)$_2$); 1.56 (s, 3H, −NHC-(CH_3)$_2$); 1.38 (s, 9H, Boc); 0.95 (d, 3H, J = 2.9 Hz, CH$_2$CH(CH_3)$_2$); 0.93 (d, 3H, J = 2.9 Hz, CH$_2$CH(CH_3)$_2$). ^{13}C NMR (δ, ppm, CDCl$_3$): 173.9; 168.7; 166.6; 154.6; 136.2; 133.8; 130.1; 128.9; 128.4; 128.0; 127.9; 127.6; 80.9; 68.8; 66.8; 60.8; 56.5; 43.6; 36.7; 28.1; 26.3; 25.6; 24.8; 23.2; 22.3. Reaction time (hydrogenation): 4 h. Yield (overall): 0.655 g (69%).

(3S,4R)-1-(3-Aza-4-carboxy-4-methyl-2-oxopentyl)-3-benzyl-3-*tert*-butoxycarbonylamino-4-isobutylazetidin-2-one (11): The general procedure was followed from (3S,4R)-3-benzyl-3-*tert*-butoxycarbonyl-amino-1-carboxymethyl-4-isobutylazetidin-2-one (**23**) (2.0 mmol, 0.781 g); eluant EtOAc/hexanes 1:2. Intermediate benzyl ester: (3S,4R)-1-(3-aza-4-benzyloxycarbonyl-4-methyl-2-oxopentyl)-3-benzyl-3-*tert*-bu-toxiaminocarbonyl-4-isobutylazetidin-2-one. [α]$^{25}_D$ = −59.2 (c = 0.52, Cl$_2$CH$_2$). IR (cm^{-1}, KBr): 3322; 3276 (NH); 2960; 1772; 1762; 1698; 1655 (C=O). ^{1}H NMR (δ, ppm, CDCl$_3$): 7.72 (s, 1H, NH); 7.39−7.24 (m, 10H, Ar); 5.17 (d, 1H, J = 12.2 Hz, OCH_2Ph); 5.12 (d, 1H, J = 12.2 Hz, OCH_2Ph); 4.66 (s, 1H, BocNH); 4.27 (d, 1H, J = 17.6 Hz, NCH_2CO); 3.73 (t, 1H, J = 6.8 Hz, NCH(^{i}Bu)); 3.27 (d, 1H, J = 17.6 Hz, NCH_2CO); 3.20 (d, 1H, J = 14.2 Hz, CCH_2Ph); 3.01 (d, 1H, J = 14.2 Hz, CCH_2Ph); 1.59 (s, 3H, NC(CH_3)$_2$(CO)); 1.60−1.52 (m, 1H, CH_2CH(CH$_3$)$_2$); 1.52 (s, 3H, NC(CH_3)$_2$(CO)); 1.46−1.42 (m, 1H, CH_2CH(CH$_3$)$_2$); 1.42 (s, 9H, Boc); 1.33−1.30 (m, 1H, CH_2CH(CH$_3$)$_2$); 0.79 (d, 3H, CH$_2$CH(CH_3)$_2$); 0.78 (d, 3H, CH$_2$CH(CH_3)$_2$). ^{13}C NMR (δ, ppm, CDCl$_3$): 173.8; 167.9; 167.4; 154.8; 136.2; 134.1; 129.8; 129.1; 128.4; 128.0; 127.8; 80.7; 70.2; 66.7; 64.3; 56.3; 53.4; 44.9; 40.5; 36.6; 28.1; 25.6; 25.4; 24.6; 22.7; 22.6. Reaction time (hydrogenation): 4 h. Yield (overall): 0.580 g (61%).

(R)-1-(3-Aza-4-benzyloxycarbonyl-2-oxobutyl)-3-benzyl-3-(2-*tert*-butoxycarbonylaminoazetidin-2-one (16). To a solution of (3R)-3-benzyl-1-carboxymethyl-3-*tert*-butoxycarbonylaminoazetidin-2-one (**5**) (1.1 mmol, 0.371 g) in dry CH$_2$Cl$_2$ (10 mL) was added EDC·HCl (1.54 mmol, 0.30 g), *p*-toluensulfonate salt of glycine benzyl ester (1.5 mmol, 0.50 g) dissolved in CH$_2$Cl$_2$ (5 mL), and Et$_3$N (3.0 mmol, 0.42 mL). The mixture was stirred at room temperature for 18 h. After this time, the solution was washed with 0.1 M HCl (6 mL × 3), saturated aqueous solution of NaHCO$_3$ (20 mL), and H$_2$O (20 mL). The organic phase was dried (MgSO$_4$) and evaporated under reduced pressure, and the resulting crude was purified by column chromatography (silica gel, eluant: EtOAc/hexanes 3:1). Yield: 0.434 g (82%).

(R)-1-(3-Aza-4-benzyloxycarbonyl-2-oxbutyl)-3-benzyl-3-(1-aza-3-*tert*-butoxycarbonylamino-2-oxopropyl)azetidin-2-one (9). To a solution of (R)-1-(3-aza-4-benzyloxycarbonyl-2-oxobutyl)-3-benzyl-3-*tert*-butoxycarbonylaminoazetidin-2-one (**16**) (0.46 mmol, 0.222 g) in dry CH$_2$Cl$_2$ (4 mL) was added trifluoroacetic acid (TFA) (13 mmol, 1.0 mL). The mixture was stirred at room temperature for 90 min, TFA was removed under reduced pressure, and the resulting residue was

dissolved in CH$_2$Cl$_2$ (10 mL). The organic solution was washed with a saturated aqueous solution of NaHCO$_3$ (20 mL × 2), dried (MgSO$_4$), and evaporated under reduced pressure to afford crude intermediate α-amino-β-lactam (0.29 mmol), which was dissolved in dry CH$_2$Cl$_2$ (3.0 mL). The mixture was cooled to 0 °C, and HOBt (0.50 mmol, 0.043 g), DMF (0.3 mL), Boc-glycine (0.50 mmol, 0.056 g), and EDC·HCl (0.69 mmol, 0.083 g) were added. The mixture was stirred at 0 °C for 1 h. After this time, the bath was removed and the solution was stirred at room temperature overnight. The reaction was treated with CH$_2$Cl$_2$ (2 mL), and the organic solution was washed successively with 0.1 M KHSO$_4$ (3 mL) and H$_2$O (3 mL), dried (MgSO$_4$), and evaporated under reduced pressure. The product was purified by chromatography (silica gel, eluant: EtOAc/hexanes 5:1). Yield (overall): 0.105 g (51%).

(3R)-1-[(Aminocarbonyl)methyl]-3-isobutyl-3-[(2S)-pyrrolidin-2-ylcarbonylamino]azetidin-2-one (13). In a flame-dried three necked round-bottomed flask fitted with a N$_2$-stream system, a condenser, and an ammonia cylinder inlett was put Li (11.9 mmol, 0.082 g; finely divided wire). Then, NH$_3$ (40 mL) was condensed (acetone, CO$_2$ bath) at −78 °C until the solution turned to deep blue and all the lithium was dissolved. A solution of (3R)-1-[(aminocarbonyl)methyl]-3-isobu-tyl-3-[(4S)-4-phenyl-2-oxooxazolidin-3-yl]azetidin-2-one (**31**) (1.98 mmol, 0.684 g) in dry THF/t-BuOH (10:1) (12 mL) was added dropwise. After the addition, the mixture was stirred at −78 °C for 5 min. Then, the flask was opened and solid NH$_4$Cl (11.9 mmol, 0.636 g) was added. The reaction mixture was left stirring at room temperature for evaporation of the NH$_3$. The solvents were evaporated, and the residue was dissolved in dry DMF (9 mL) and introduced in a flamed round-bottomed flask under N$_2$. To this solution were added Cbz-Pro-fluoride (2.97 mmol, 0.745 g) in dry CH$_2$Cl$_2$ (3 mL) and N-methylmorpholine (5.94 mmol, 0.69 mL). The mixture was stirred at room temperature for 8 h, and CH$_2$Cl$_2$ (15 mL) was added. The resulting solution was successively washed with H$_2$O (10 mL), 1 M HCl (10 mL), and a saturated aqueous NaHCO$_3$ (10 mL). The organic layer was decanted and dried (MgSO$_4$), and the solvents were evaporated under reduced pressure. The intermediate (3R)-1-[(aminocarbonyl)-methyl]-3-isobutyl-3-[(2S)-1-(benzyloxycarbonyl)pyrrolidin-2-ylcarbo-nylamino]azetidin-2-one was purified by column chromatography (silica gel; CH$_2$Cl$_2$/MeOH 95:5). Yield (overall from **31**): 0.443 g (52%). [α]$^{25}_D$ = −44.8 (c = 0.59, Cl$_2$CH$_2$). IR (cm^{-1}, KBr): 3392.7; 3181.2 (NH); 2955.2; 2922.7; 2869.0; 1750.0; 1687.9; 1667.0 (CO). MS m/z (int): 91 (100); 160 (39.3); 288 (11.0); 330 (6.6); 429 (16.6); ^{1}H NMR (δ, ppm, CDCl$_3$): 8.21 (s, 1H, −NHCO); 7.70 (s 1H, −CONH_2); 7.37 (s, 5H, Ar); 5.48 (s, 1H, −CONH_2); 5.17 (m, 2H, PhCH_2O); 4.47 (d, 1H, J = 18.1 Hz, −NCH_2C−); 4.39 (s$_b$, 1H, Cbz-NCHCH$_2$−); 3.79 (s$_b$, 1H, −NCH_2CONH$_2$); 3.50 (s$_b$, 2H, Cbz-NCH_2CH$_2$−); 3.43 (d, 1H, J = 17.6 Hz, −NCH_2C−); 3.30 (s$_b$, 1H, −NCH_2CONH$_2$); 1.93 (m, 5H, CbzNCH$_2$CH_2−; CH_2CH(CH$_3$)$_2$); 1.57 (m, 2H, CbzNCHCH_2−); 1.00 (s$_b$, 3H, CH$_2$CH(CH_3)$_2$); 0.90 (d, 3H, J = 6.4 Hz, CH$_2$CH(CH_3)$_2$). ^{13}C NMR (δ, ppm, CDCl$_3$): 171.7; 170.3; 168.4; 156.8; 136.2; 128.6; 128.3; 127.9; 68.2; 67.6; 60.1; 53.2; 47.2; 44.9; 42.2; 26.9; 24.6; 23.8; 22.4. A suspension of this compound (1.0 mmol, 0.430 g) and (10%) Pd/C (0.1 mmol, 0.10 g) in EtOH (10 mL) was stirred at room temperature for 24 h under hydrogen (1 atm.). The solution was filtered through a pad of Celite (washed several times with CH$_2$Cl$_2$), and the solvents were evaporated under reduced pressure to afford pure product. Yield (hydrogenolysis): 100%. Yield (overall from **31**): 0.305 g (52%).

General Procedure for the α-Alkylation of 4-Alkyl(aryl)-1-[bis-(trimethylsilyl)methyl]-3-[(4S)-4-phenyl-2-oxooxazolidin-3-yl]azeti-din-2-ones. Synthesis of 18, 26, 27, 28, and 29. To a suspension of 1,10-phenantroline (2 mg, indicator) in anhydrous THF (16 mL) cooled to −78 °C under nitrogen atmosphere was added 2.5 M n-BuLi dropwise until a dark red color was observed (usually 2 or 3 drops). Dry diisopropylamine (12.0 mmol, 1.68 mL) and 2.5 M n-BuLi (12.0 mmol, 4.8 mL) were added, and the mixture was stirred at −78 °C for 30min. A solution of the corresponding 4-alkyl(aryl)-1-[bis(trimethyl-silyl)methyl]-3-[(4S)-4-phenyl-2-oxooxazolidin-3-yl]azetidin-2-one (8.0

mmol) in anhydrous THF (24 mL) was added dropwise, and the stirring was continued for 1 h at −78 °C. Freshly distilled alkyl bromide (40.0 mmol) was added slowly, and the dry ice/acetone bath was allowed to reach room temperature overnight. The reaction mixture was taken up over CH₂Cl₂ (65 mL), washed successively with aqueous saturated NH₄-Cl (32 mL × 2), 1 M HCl (20 mL), saturated aqueous NaHCO₃ (20 mL), and H₂O (20 mL × 2), dried (MgSO₄), and evaporated at reduced pressure. The products were purified by column chromatography (silica gel, eluant: EtOAc/hexanes).

(3*R*,4*R*)-3-Benzyl-1-[bis(trimethylsilyl)methyl]-4-isobutyl-3-[(4*S*)-4-phenyl-2-oxooxazolidin-3-yl]azetidin-2-one (18). The general procedure was followed from (3*S*,4*R*)-1-[bis(trimethylsilyl)methyl]-4-isobutyl-3-[(4*S*)-4-phenyl-2-oxooxazolidin-3-yl]-azetidin-2-one (17) (8.0 mmol, 3.57 g) and benzyl bromide (40.0 mmol, 4.86 mL). Eluant: EtOAc/hexanes 1:10. Yield: 3.56 g (83%).

(3*R*,4*R*)-3-Allyl-1-[bis(trimethylsilyl)methyl]-4-isobutyl-3-[(4*S*)-4-phenyl-2-oxooxazolidin-3-yl]azetidin-2-one (26). The general procedure was followed using a 1/10 scale from (3*S*,4*R*)-1-[bis(trimethylsilyl)methyl]-4-isobutyl-3-[(4*S*)-4-phenyl-2-oxooxazolidin-3-yl]azetidin-2-one (17) (0.8 mmol, 0.357 g) and allyl bromide (4.0 mmol, 0.352 mL). Eluant: EtOAc/hexanes 1:5. Yield: 0.194 g (50%).

(3*R*,4*R*)-1-[Bis(trimethylsilyl)methyl]-3-(4-bromobenzyl)-4-ethyl-3-[(4*S*)-4-phenyl-2-oxooxazolidin-3-yl]azetidin-2-one (27). The general procedure was followed using a 1/10 scale from (3*S*,4*R*)-1-[bis(trimethylsilyl)methyl]-4-ethyl-3-[(4*S*)-4-phenyl-2-oxooxazolidin-3-yl]azetidin-2-one (24) (0.8 mmol, 0.329 g) and 4-bromobenzyl bromide (4.0 mmol, 0.586 mL). Eluant: EtOAc/hexanes 1:5. Yield: 0.282 g (60%).

(3*R*,4*R*)-1-[Bis(trimethylsilyl)methyl]-3-(2-methyl-2-propenyl)-4-phenyl-3-[(4S)-4-phenyl-2-oxooxazolidin-3-yl]azetidin-2-one (28). The general procedure was followed using a 1/10 scale from (3*S*,4*R*)-1-[bis(trimethylsilyl)methyl]-4-phenyl-3-[(4*S*)-4-phenyl-2-oxooxazolidin-3-yl]azetidin-2-one (25) (0.8 mmol, 0.373 g) and methallyl bromide (4.0 mmol, 0.416 mL). Eluant: EtOAc/hexanes 1:4. Yield: 0.242 g (58%).

(3*R*,4*R*)-1-[Bis(trimethylsilyl)methyl]-3-(2-methyl-2-propenyl)-4-phenyl-3-[(4*S*)-4-phenyl-2-oxooxazolidin-3-yl]azetidin-2-one (29). The general procedure was followed using a 1/10 scale from (3*S*,4*R*)-1-[bis(trimethylsilyl)methyl]-4-phenyl-3-[(4*S*)-4-phenyl-2-oxooxazolidin-3-yl]azetidin-2-one (25) (0.8 mmol, 0.373 g) and 4-methylbenzyl bromide (4.0 mmol, 0.752 mL). Eluant: EtOAc/hexanes 1:4. Yield: 0.333 g (80%).

(3*R*,4*R*)-3-Benzyl-3-*tert*-butoxycarbonylamino-4-isobutyl-azetidin-2-one (19). In a flame-dried three-necked round-bottomed flask fitted with a N₂-stream system, a condenser, and an ammonia cylinder inlett was put Li (72.0 mmol, 0.50 g; finely divided wire). Then, NH₃ (190 mL) was condensed (acetone, CO₂ bath) at −78 °C until the solution turned to deep blue and all the lithium was dissolved. A solution of (3*R*,4*R*)-3-benzyl-1-[bis(trimethylsilyl)methyl]-4-isobutyl-3-[(4*S*)-4-phenyl-2-oxooxazolidin-3-yl]azetidin-2-one (18) (12.0 mmol, 6.44 g) in dry THF/*t*-BuOH (10:1) (65 mL) was added dropwise. After the addition, the mixture was stirred at −78 °C for 5 min, the flask was opened, and solid NH₄Cl (72.0 mmol, 3.90 g) was added. The reaction mixture was left stirring at room temperature overnight until complete evaporation of ammonia. The solvents were evaporated under reduced pressure, and the residue was dissolved in H₂O (190 mL), acidified with 6 M HCl to pH = 3−4, and basified with aqueous 40% NaOH to pH = 10. The product was extracted with CH₂Cl₂ (130 mL × 3), the organic phase was dried (MgSO₄), and the solvents were removed under reduced pressure. The resulting crude (11.9 mmol) was dissolved in CH₂Cl₂ (50 mL), di-*tert*-butyl dicarbonate (23.8 mmol, 5.35 g) was added, and the solution was stirred at room temperature for 22 h. It was washed successively with H₂O (22 mL), 20% NaHSO₃ (22 mL), and saturated aqueous NaHCO₃ (22 mL), dried (MgSO₄) and evaporated under reduced pressure. The intermediate (3*R*,4*R*)-3-benzyl-1-[bis(trimethylsilyl)methyl]-3-*tert*-butoxycarbonylamino-4-isobutylazetidin-

2-one was purified by column chromatography (silica gel; eluant: EtOAc/hexanes 1:200, then 1:100, and finally 1:50). Yield (overall from **18**): 5.24 g (89%). [α]²⁵_D = +3.11 (*c*= 0.96, Cl₂CH₂). IR (cm⁻¹, KBr): 2943.0 (NH); 1742.2, 1717.0 (C=O). ¹H NMR (δ, ppm, CDCl₃): 7.31−7.21 (m, 5H, Ar); 4.97 (s, 1H, NH); 3.76 (t, 1H, *J* = 6.5 Hz, CC*H*N); 3.36 (d, 1H, *J* = 13.7 Hz, C*H*₂Ph); 2.93 (d, 1H, *J* = 13.7 Hz, C*H*₂Ph); 2.08 (s_b, 2H, C*H*(CH₃)₂, C*H*(SiMe₃)₂); 1.72−1.52 (m, 1H, C*H*₂CH(CH₃)₂); 1.50−1.41 (m, 1H, C*H*₂CH(CH₃)₂); 1.41 (s, 9H, Boc); 1.03 (t, 6H, *J* = 6.6 Hz, CH(C*H*₃)₂); 0.22 (s, 9H, Si(C*H*₃)₃); 0.15 (s, 9H, Si(C*H*₃)₃). ¹³C NMR (δ, ppm, CDCl₃): 166.9; 154.5; 135.8; 130.4; 127.9; 126.5; 79.3; 67.1; 65.0; 37.9; 36.9; 35.0; 28.1; 25.2; 22.8; 22.7; 0.0. To a solution of this product (10.7 mmol, 5.24 g) in dry acetonitrile (50 mL) cooled to 0 °C was added a solution of Ce(NH₄)₂-(NO₃)₄ (45.9 mmol, 25.2 g) in H₂O (30 mL), and the mixture was stirred at 0 °C for 2 h (TLC). EtOAc (100 mL) and H₂O (50 mL) were added, and the organic layer was separated, washed with saturated aqueous NaHCO₃ (50 mL), dried (MgSO₄), and evaporated under reduced pressure. The crude intermediate (3*R*,4*R*)-3-benzyl-1-formyl-3-*tert*-butoxycarbonylamino-4-isobutyl-3-azetidin-2-one was dissolved in a mixture of methanol (33 mL), saturated aqueous NaHCO₃ (33.5 mL), and Na₂CO₃ (5.3 mmol, 0.56 g) ,and the suspension was stirred at room temperature for 2 h. Then, H₂O (40 mL) was added, the solution was extracted with CH₂Cl₂ (25 mL × 2), and the organic layer was dried (MgSO₄) and evaporated in vacuo. The product was purified by column chromatography (silica gel, eluant EtOAc/hexanes 1:3). Yield (overall from **18**): 4.07 g (76%).

(3*S*,4*R*)-3-Benzyl-3-benzylideneamino-4-isobutyl-1-[bis(trimethylsilyl)methyl]azetidin-2-one (21). In a flame-dried three-necked round-bottomed flask fitted with a N₂-stream system, a condenser, and an ammonia cylinder inlett, was put Li (30.6 mmol, 0.21 g; finely divided wire). Then, NH₃ (90 mL) was condensed (acetone, CO₂ bath) at −78 °C until the solution turned to deep blue and all the lithium was dissolved. A solution of (3*S*,4*R*)-1-[bis(trimethylsilyl)methyl]-4-isobutyl-3-[(4*S*)-4-phenyl-2-oxooxazolidin-3-yl]azetidin-2-one (17) (5.1 mmol, 2.03 g) in dry THF/*t*-BuOH (10:1) (28 mL), was added dropwise. After the addition the mixture was stirred at −78 °C for 5 min, the flask was opened and solid NH₄Cl (30.6 mmol, 1.63 g) was added. The reaction mixture was left stirring at room temperature overnight until the complete evaporation of ammonia. The solvents were evaporated under reduced pressure and the residue was dissolved in H₂O (85 mL), acidified with 6 M HCl to pH = 3−4, and basified with aqueous 40% NaOH to pH = 10. The intermediate α-amino-β-lactam was extracted with CH₂Cl₂ (60 mL × 3), the organic phase was dried (MgSO₄) and the solvents were removed under reduced pressure. To a solution of this crude (5.0 mmol) in dry CH₂Cl₂ (15 mL) under nitrogen atmosphere and with molecular sieves (4 Å; 2 g) was added benzaldehyde (5.0 mmol, 0.5 mL), and the mixture was stirred at room temperature for 1 h. After this time the molecular sieves were filtered and the solvents were evaporated. The crude benzaldimine was used without further purification. To a suspension of 1,10-phenantroline (2 mg, indicator) in anhydrous THF (40 mL) under nitrogen atmosphere and cooled to −78 °C 2.5 M *n*-BuLi in hexane was added dropwise until dark red color was observed (usually 2 or 3 drops). Dry DIPA (5.44 mmol, 0.78 mL) and 2.5 M *n*-BuLi (5.40 mmol, 2.16 mL) were added, and the mixture was stirred at −78 °C for 30 min. A solution of (3*S*,4*R*)-3-benzylideneamino-4-isobutyl-1-[bis(trimethylsilyl)methyl]-azetidin-2-one (4.53 mmol, 1.76 g) in dry THF (40 mL) was added dropwise and stirring was continued for 1 h at −78 °C. After this time, freshly distilled benzyl bromide (13.5 mmol, 1.61 mL) was added slowly, and the reaction mixture was stirred to room temperature overnight. The solution was diluted with CH₂Cl₂ (45 mL), washed successively with saturated aqueous NH₄Cl (25 mL), 1 M HCl (8 mL), and saturated aqueous NaHCO₃ (25 mL), dried (MgSO₄), and evaporated. The product was used without further purification. Yield (overall from **17**): 1.295 g (53%).

(3*R*, 4*R*)-3-Benzyl-3-*tert*-butoxycarbonylamino-4-isobutyl-azetidin-2-one (22). To a solution of crude (3*S*,4*R*)-3-benzyl-3-benzylideneamino-4-isobutyl-1-[bis(trimethylsilyl)methyl]azetidin-2-one (**21**) (5.0 mmol, 1.94 g) in Et₂O (50 mL) and H₂O (0.3 mL) cooled to 0 °C (ice bath) was added strongly acidic Amberlist-15 resin (15 g; pH < 3), and the mixture was stirred at room temperature for 1 h (monitored by TLC until complete imine consumption). The resin was filtered and suspended in CH₂Cl₂ (60 mL), hexamethyldisilazane (20 mL) was added, and the suspension was stirred overnight. The resin was filtered off, and the solvents were evaporated under reduced pressure to afford crude(3*R*,4*R*)-3-amino-3-benzyl-4-isobutyl-1-[bis(trimethylsilyl)methyl]azetidin-2-one which was dissolved in *t*-BuOH (40 mL) under nitrogen. To this solution were added tri(*n*-butyl)phosphine (1.0 mmol, 0.200 g) and (Boc)₂O (10 mmol, 2.30 g), the mixture was stirred at 70 °C for 24 h, and the *t*-BuOH was evaporated under reduced pressure. The intermediate (3*S*,4*R*)-3-benzyl-1-[bis(trimethylsilyl)methyl]-3-*tert*-butoxycarbonylamino-4-isobutylazetidin-2-one was purified by column chromatography (silica gel; eluant: EtOAc/hexanes 1:50, then 1:20, then 1:10 and finally 1:5). Yield (overall from **21**): 1.34 g (60%). [α]$^{25}_D$ = +3.04 (*c* = 0.92, Cl₂CH₂). IR (cm⁻¹, KBr): 1702.9; 1731.8 (C= O). ¹H NMR (δ, ppm, CDCl₃): 7.34−7.20 (m, 5H, Ar); 4.84 (s, 1H, N*H*Boc); 3.59−3.54 (d, m, 2H, C*H*₂Ph y *H*C(ⁱBu)); 3.29 (d, 1H, *J* = 13.7 Hz, C*H*₂Ph); 2.00 (s, 1H, C*H*(Si(CH₃)₃)₂); 1.80−1.78 (m, 1H, CH₂C*H*(CH₃)₂); 1.60−1.55 (m, 1H, C*H*₂CH(CH₃)₂); 1.42 (s, 9H, OCOC(C*H*₃)₃); 1.35−1.27 (m, 1H, C*H*₂CH(CH₃)₂); 0.94 (s, 3H, CH₂-CH(C*H*₃)₂); 0.93 (s, 3H, CH₂CH(C*H*₃)₂); 0.17 (s, 9H, Si(C*H*₃)₃); 0.07 (s, 9H, Si(C*H*₃)₃). ¹³C NMR (δ, ppm, CDCl₃): 166.4; 154.4; 135.9; 130.6; 130.5; 128.4; 128.2; 126.7; 79.6; 69.3; 64.1; 39.0; 37.0; 36.9; 36.4; 28.2; 27.8; 25.4; 23.2; 22.7; 0.09; −0.13. To a solution of this product (3.0 mmol, 1.34 g) in dry acetonitrile (20 mL) cooled to 0 °C was added a solution of Ce(NH₄)₂(NO₃)₄ (13.5 mmol, 7.40 g) in H₂O (10 mL). and the mixture was stirred at 0 °C for 2 h (TLC). EtOAc (100 mL) and H₂O (50 mL) were added, and the organic layer was separated, washed with saturated aqueous NaHCO₃ (50 mL), dried (MgSO₄), and evaporated under reduced pressure. The crude intermediate (3*S*,4*R*)-3-benzyl-1-formyl-3-*tert*-butoxycarbonylamino-4-isobutyl-3-azetidin-2-one was dissolved in a mixture of methanol (30 mL), saturated aqueous NaHCO₃ (30 mL), and Na₂CO₃ (3 mmol, 0.32 g), and the suspension was stirred at room temperature for 2 h. Then, H₂O (40 mL) was added, the solution was extracted with CH₂Cl₂ (20 mL × 2), and the organic layer was dried (MgSO₄) and evaporated in vacuo. The product was purified by column chromatography (silica gel, eluant EtOAc/hexanes 1:2). Yield (overall from **21**): 0.860 g (52%).

(3*R*)-1-[Bis(trimethylsilyl)methyl]-3-isobutyl-3-[(4*S*)-4-phenyl-2-oxooxazolidin-3-yl]azetidin-2-one (30). To a suspension of 1,10-phenanthroline (2 mg, indicator) in anhydrous THF (32 mL) cooled to −78 °C under nitrogen atmosphere was added 2.5 M *n*-BuLi dropwise until a dark red color was observed (usually 2 or 3 drops). Dry diisopropylamine (20.0 mmol, 2.70 mL) and 2.5 M *n*-BuLi (20.0 mmol, 8.0 mL) were added, and the mixture was stirred at −78 °C for 30 min. A solution of (3*S*)-1-[bis(trimethylsilyl)methyl]-3-[(4*S*)-4-phenyl-2-oxo-1,3-oxazolidin-3-yl]azetidin-2-one (**4**) (16.0 mmol, 6.30 g) in anhydrous THF (32 mL) was added dropwise, and the stirring was continued for 30 min at −78 °C. After this time, freshly distilled 3-bromo-2-methylpropene (80.0 mmol, 8.35 mL) was added slowly and the dry ice/acetone bath was allowed to reach room temperature overnight. The reaction mixture was taken up over CH₂Cl₂ (65 mL), washed successively with aqueous saturated NH₄Cl (32 mL × 2) and H₂O (20 mL × 2), dried (MgSO₄), and evaporated at reduced pressure. The intermediate (3*R*)-1-[bis(trimethylsilyl)methyl]-3-[2-methyl-2-propenyl]-3-[(4*S*)-4-phenyl-2-oxooxazolidin-3-yl]azetidin-2-one was purified by column chromatography (silica gel, eluant: EtOAc/hexanes 1:8). [α]$^{25}_D$ = +0.8 (*c* = 1.0, Cl₂CH₂). IR (cm⁻¹, KBr): 1740 (CO). MS *m/z* (int): 45 (27.2); 73 (100); 80 (23.3); 104 (100); 165 (39.6); 229 (100); 244 (25.3). ¹H NMR (δ, ppm, CDCl₃): 7.35 (m, 3H, Ph); 7.57 (m, 2H, Ph); 5.13 (dd, 1H, *J* = 8.1; 1.9 Hz, OC*H*HCHPh); 4.80 (s,

1H, HC*H*=); 4.72 (s, 1H, *H*CH=); 4.59 (t, 1H, *J* = 8.4 Hz, *H*CPh); 4.40 (dd, 1H, *J* = 8.6, 1.9 Hz, OCH*H*CHPh); 3.62 (d, 1H, *J* = 6.5 Hz, HC*H*N); 3.57 (d, 1H, *J* = 6.5 Hz, *H*CHN); 2.73 (s, 1H, C*H*Si); 2.33 (d, 1H, *J* = 13.7 Hz, CH₂C=); 1.61 (d, 1H, *J* = 13.7 Hz, CH₂C=); 1.57 (s, 3H, CH₃); 0.15 (s, 9H, (CH₃)₃); 0.12 (s, 9H, (CH₃)₃). ¹³C NMR (δ, ppm, CDCl₃): 164.8; 156.6; 140.1; 139.6; 129.1; 128.9; 127.8; 116.2; 71.1; 70.6; 59.6; 52.9; 39.4; 37.1; 23.8; −0.3. This product was dissolved in EtOH (20 mL) containing 10% Pd/C (0.50 g), and the mixture was stirred for 24 h under hydrogen atmosphere (1 atm) at room temperature. After this time, the suspension was filtered through a pad of Celite and washed with CH₂Cl₂ (20 mL × 2), and the combined organic solution evaporated under reduced pressure to afford pure product. Yield (overall): 5.50 g (77%).

(3*R*)-1-[(Aminocarbonyl)methyl]-3-isobutyl-3-[(4*S*)-4-phenyl-2-oxooxazolidin-3-yl]azetidin-2-one (31). A 0.60 M solution of *n*-BuLi/TMEDA in THF was prepared under nitrogen by adding dried TMEDA (12 mmol, 1.8 mL) and 2.5 M *n*-BuLi (12 mmol, 4.8 mL) to anhydrous THF (13.0 mL) cooled to −100 °C (MeOH/N₂ bath). In another flask, a solution of (3*R*)-1-[bis(trimethylsilyl)methyl]-3-isobutyl-3-[(4*S*)-4-phenyl-2-oxooxazolidin-3-yl]azetidin-2-one (**30**) (4 mmol, 1.79 g) was dissolved in anhydrous THF (12 mL) and cooled to −100 °C under nitrogen, and *n*-BuLi/TMEDA (0.60 M solution in THF, 4.8 mmol, 8.0 mL) was added dropwise. The mixture, which turned to a red-orange color, was stirred at −100 °C for 30 min. Then, trimethylsilyl isocyanate (12 mmol, 1.60 mL) was added, and the mixture was stirred at −78 °C for 2 h. The reaction mixture was quenched at low temperature (−78 °C) with saturated aqueous NH₄Cl (16 mL) and left to reach room temperature by removing the cooling bath. Extraction with CH₂Cl₂ (20 mL × 3), drying (MgSO₄), evaporation, and purification by column chromatography (silica gel, eluant: EtOAc 100%) afforded the product. Yield: 1.10 g (80%).

(3*R*)-1-Amidomethyl-3-isobutyl-3-[(2*S*)-1-(*tert*-butoxycarbonyl)-pyrrolidin-2-ylcarbonylamino]azetidin-2-one (32). A solution of (3*R*)-1-amidomethyl-3-isobutyl-3-[(2*S*)-pyrrolidin-2-ylcarbonylamino]azetidin-2-one (**13**) (1 mmol, 0.296 g) and di-*tert*-butyl dicarbonate (2 mmol, 0.436 g) in THF (3.0 mL) was stirred at room temperature for 16 h and then was poured into a mixture of CH₂Cl₂ (20 mL) and H₂O (5 mL). The organic layer was washed successively with H₂O (10 mL), 20% NaHSO₃ (10 mL), and saturated aqueous NaHCO₃ (10 mL), dried (MgSO₄), and evaporated under reduced pressure. The product was purified by column chromatography (silica gel, eluants: EtOAc/hexanes 1:10, then, CH₂Cl₂/MeOH 90:10). Yield: 0.368 g (93%).

Molecular Dynamics of Compounds 6, 8, 9, 10, 11, 12, and 13. MD simulations were carried out at 300 K and 1 atm using the SANDER module in AMBER 6. The updated (parm99) second-generation[48] AMBER force field[49] was used. Each compound was immersed in a periodic box of ∼160 DMSO[50] molecules that extended up to 10 Å away from any solute atom. Periodic boundary conditions were applied. A dielectric constant of 1 was used, and the cutoff distance for the nonbonded interactions was 10 Å. The geometries of the molecules were fully optimized with the ab initio quantum mechanical program Gaussian 98[51] at the Hartree−Fock level using the 3-21G(d) basis set. Partial atomic charges were then obtained using the RESP[52] methodology with the 6-31G(d) basis set. SHAKE[53] was applied to all bonds involving hydrogen atoms, and the integration time step was 1 fs. The simulation protocol consisted of a series of progressive energy

(48) Cornell, W. D.; Cieplak, P.; Bayly, C. I.; Gould, I. R.; Merz, K. M.; Ferguson, D. M.; Spellmeyer, D. C.; Fox, T.; Caldwell, J. W.; Kollman, P. A. A second generation force field for the simulation of proteins, nucleic acids, and organic molecules. *J. Am. Chem. Soc.* **1995**, *117*, 5179−5197.
(49) Case, D. A.; Pearlman, D. A.; Caldwell, J. W.; Cheatham, T. E., III; Ross, W. S.; Simmerling, C. L.; Darden, T. A.; Merz, K. M.; Stanton, R. V.; Cheng, A. L.; Vincent, J. J.; Crowley, M.; Tsui, V.; Radmer, R. J.; Duan, Y.; Pitera, J.; Massova, I.; Seibel, G. L.; Singh, U. C.; Weiner, P. K.; Kollman, P. A. AMBER 6; University of California, San Francisco, 1999.
(50) The molecular structure of DMSO was optimized until the experimentally measured density and heat of vaporization of this liquid were produced, thereby lending credence to the suitability of the parameters that were used in the simulations (see the Supporting Information).

minimizations followed by a 20 ps heating phase and a 400 ps equilibration period during which distance restraints (10 kcal mol^{-1} Å^{-2}) were applied to maintain the $_{(i)}$C=$O\cdots$H-$N_{(i+3)}$ distance (2.8 ± 0.1 Å) as this hydrogen bond characterizes the β-turn. This restraint was removed thereafter and the system coordinates were then collected every picosecond for 5 ns which yielded an ensemble of 5000 structures for each peptide for further analysis.

RMN/X-PLOR Annealing Study of Compounds 6, 8, 9, 10, 11, and 13. Upper-bonded interproton distances were calculated from NOESY intensities (see the Supporting Information, Table S1), and a hybrid distance geometry-simulated annealing method was applied using the program X-PLOR-NIH 2.0.6.[43] The MD protocol sa.inp[54] was used with modified parallhdg.pro and topallhdg.pro files with the following settings: 10000 steps at 700 K (step time 1.5 fs) and subsequent cooling in 5000 steps to 300 K. The NOE and DIHE scales were set, respectively, to 50 and 5.0, and a soft-square potential was used. All other parameters were left unchanged.

Biological Evaluation of Compounds 12 and 13 as Dopaminergic D$_2$ Receptor Agonists on Cultured Neurons. Neuronal Culture Preparation. Rat cerebral cortex[55] were obtained as previously described[47] with minor modifications. After cerebral cortex removal from E17 rat brains, tissue was treated with 0.2% trypsin plus 0.02%

DNAse in Hank's balanced salt solution during 5 min at 37 °C. After stopping enzymatic reaction, tissue was further homogenized by mechanical pippeting. Neurons were seeded into 24-well plates bearing 12-mm diameter coverslips coated with poly-D-lysine (10 μg/mL) at a density of 3×10^5 cells/well in Neurobasal medium (Gibco) supplemented with B27, 0.5 mM glutamine, 1000 U/mL of penicillin, and 100 μg/mL of streptomycin.

[^{3}H]Spiroperidol/N-Propylnorapomorphine (NPA) Binding Competition Assay. Cells were incubated with 0.5 nM [^{3}H]spiroperidol and varying concentrations of N-propylnorapomorphine (NPA) for 1 h at room temperature in a total volume of 0.5 mL. The reaction was finished by rapid wash in ice-cold buffer, and the retained radioactivity was counted after lysing cells with 0.1 N NaOH plus 0.01% Triton X-100. Nonspecific binding was determined by performing the assay in the presence of 1 μM (+)-butaclamol. Concentration of [^{3}H]spiroperidol in competitive binding assay was near its affinity constant ($K_d = 0.99$ nM) as previously determined by saturation binding experiments. The binding data were analyzed using the nonlinear curve-fitting Prism program (Graph Pad Software, San Diego, CA).[56] The IC$_{50}$ values obtained from the competition curves were converted to K_i using the Cheng and Prusoff equation. Data were expressed as mean ± sem. Statistical differences between inhibitor constant were analyzed with ANOVA with repeated measurements ($p < 0.05$; $n = 5$ in triplicate).

Supporting Information Available: Analytical and spectral characterization data of all new compounds, NMR/NOESY interprotonic distances, and crystallographic data (CIF). This material is available free of charge via the Internet at http://pubs.acs.org.

JA038180A

(51) Frisch, M. J.; Trucks, G. W.; Schlegel, H. B.; Scuseria, G. E.; Robb, M. A.; Cheeseman, J. R.; Zakrzewski, V. G.; Montgomery, J. A., Jr.; Stratmann, R. E.; Burant, J. C.; Dapprich, S.; Millam, J. M.; Daniels, A. D.; Kudin, K. N.; Strain, M. C.; Farkas, O.; Tomasi, J.; Barone, V.; Cossi, M.; Cammi, R.; Mennucci, B.; Pomelli, C.; Adamo, C.; Clifford, S.; Ochterski, J.; Petersson, G. A.; Ayala, P. Y.; Cui, Q.; Morokuma, K.; Malick, D. K.; Rabuck, A. D.; Raghavachari, K.; Foresman, J. B.; Cioslowski, J.; Ortiz, J. V.; Stefanov, B. B.; Liu, G.; Liashenko, A.; Piskorz, P.; Komaromi, I.; Gomperts, R.; Martin, R. L.; Fox, D. J.; Keith, T.; Al-Laham, M. A.; Peng, C. Y.; Nanayakkara, A.; Gonzalez, C.; Challacombe, M.; Gill, P. M. W.; Johnson, B. G.; Chen, W.; Wong, M. W.; Andres, J. L.; Head-Gordon, M.; Replogle, E. S.; Pople, J. A. *Gaussian 98*; Gaussian, Inc.: Pittsburgh, PA, 1998.
(52) Bayly, C. I.; Cieplak, P.; Cornell, W. D.; Kollman, P. A. A *J. Phys. Chem.* **1993**, *97*, 10269−10280.
(53) Ryckaert, J. P.; Ciccoti, G.; Berendsen, H. J. C. *J. Comput. Phys.* **1977**, *23*, 327−341.
(54) Nilges, M.; Kuszewski, J.; Brunger, A. T.; Hoch, J. C.; Poulsen, F. M.; Redfield, C. Ed.; Plenum Press: New York, 1991.
(55) This region was selected because is highly enriched in D$_2$ receptors and yields sufficient cells for culture experiments: Khan, Z. U.; Koulen, P.; Rubinstein, M.; Grandy, D. K.; Goldman-Rakic, P. S. *Proc. Natl. Acad. Sci. U.S.A.* **2001**, *98*, 1964−1969.

(56) Cheng, Y. C.; Prusoff, W. H. *Biochem. Pharmacol.* **1973**, *22*, 3099−3108.